PURDUE
UNIVERSITY

DEPARTMENT OF CHEMISTRY

Dear Dr. Laskin,

In this document, we provide our revised manuscript, "Nitrate radical oxidation of γ-terpinene: hydroxy nitrate, total organic nitrate, and secondary organic aerosol yields", and a point-by-point response to the very careful and thoughtful critiques by the three anonymous referees, in the order the comments were raised. We believe we have satisfactorily responded to all referee comments, which has resulted in a significantly improved manuscript. While no changes were made to our original conclusions, the revised manuscript highlights and expands on relevant gas-phase HO_2 chemistry, secondary oxidation reactions, and potentially novel chemistry involving peroxyacyl nitrate epoxidation of olefins in the particle phase, further underscoring the importance of polyolefinic monoterpenes in SOA formation and chemistry. We believe the results presented in this manuscript will make a valuable contribution to the current literature and promote future studies on polyolefinic monoterpene oxidation. We hope you agree that our manuscript is in publishable form.

Our responses to each reviewer comment is provided below showing the reviewer comment in *italics* and reviewer response in normal font. Changes to the manuscript resulting from each reviewer comment are specified in each response to the reviewer by section and line number of the revised manuscript. Additions or modifications to the manuscript are indicated in bold font in the revised manuscript found at the bottom of this document.

We hope you agree that we have completely responded to all reviewer comments and that the paper is now in suitable form for publication. Thank you very much for your consideration.

Sincerely yours,

Jonathan H. Slade Jr., Ph.D.

Department of Chemistry
Brown Laboratory of Chemistry Building • 560 Oval Drive • West Lafayette, IN 47907-2084

RESPONSES TO ANONYMOUS REVIEWER #1

The authors greatly appreciate the comments and careful critique by reviewer #1, which have improved the quality of the manuscript. Below we provide a point-by-point response (shown in normal font) to the reviewer's comments (shown in italic font). Corresponding changes to the manuscript are shown in bold font of the revised version of our manuscript and indicated here based on line number.

Reviewer comment #1: *on p. 5 around line 85: Perhaps worth mentioning some other measurements of organic nitrate aerosol in the western US, by TD-LIF at BEACHON 2011 in the Colorado front range (http://www.atmos-chem-phys.net/13/8585/2013/), in various locations by FTIR (http://www.pnas.org/content/108/9/3516.full), and at Blodgett (http://www.atmoschem-phys.net/12/5773/2012/acp-12-5773-2012.pdf). In the first two cases, they are surely likely to be multifunctional, and in the latter case the authors explicitly measure multifunctional nitrates. So I'd avoid the statement that these types of molecules have only been measured in the eastern US.*

Author response to reviewer comment #1: We thank the reviewer for providing these references. They have been included in the revised version of the manuscript in lines 87-94.

Reviewer comment #2: *General comment: your chamber experiment likely has RO2 + NO3 (or RO2+RO2 where VOC » N2O5) as the dominant fate of the RO2 radical, which may bias to a particular product set. Given that ambient nighttime chemistry may have substantially more RO2 + HO2 reactions, maybe it's worth speculating on how that would affect your conclusions about partitioning implications.*

Author response to reviewer comment #2: We appreciate the reviewer's suggestion here as our chamber conditions may not represent conditions of all nighttime ambient forest environments. Given that ambient nighttime chemistry may have significantly more RO_2+HO_2 reactions, it is likely that the organic nitrate product distribution in ambient nighttime air is weighted more towards nitrooxy hydroperoxides. We have included a discussion of the impact of relative amounts of HO_2 between our chamber experiments and the ambient environment in sec. 3.3, lines 345-354 in the revised manuscript. We have also updated Fig. 9 (new Fig. 10) to show the evolution in the modeled ratio of NO_3/HO_2 and comparison to with ratios measured in the field.

Reviewer comment #3: *p. 11 line 213-214, maybe reference Ng et al 2017 instead of Fry et al 2014, since Ng reviews all lit on NO3 + a-pinene. http://www.atmos-chem-phys.net/17/2103/2017/acp- 17-2103-2017.pdf.*

Author response to reviewer comment #3: Thank you. We have instead referenced Ng et al., [2017].

Reviewer comment #4: *p. 11, line 217: "and likely g-terpinene, lose the nitrate moeity and hence are sufficiently volatile. . ."*

Author response to reviewer comment #4: This sentence has been modified accordingly in sec. 3.1, line 237 of the revised manuscript.

Reviewer comment #5: *p. 12: why would oxidation of 2nd double bond remove observed ON? Wouldn't this just double the amount of ON detected since you see each functional group and now there are 2 nitrate fxnal groups? The discussion of the secondary oxidation here is a bit confusing.*

Author response to reviewer comment #5: We thank the reviewer for highlighting this point. The expected first-generation oxidation products of γ-terpinene oxidation by NO_3 have a remaining double bond intact. Thus second-generation oxidation would likely occur at the position of the remaining double bond, potentially producing a second nitrate functionality, and therefore increase our FTIR-derived ON concentrations instead of decreasing them.

We have clarified in the methods section, lines 164-172, the potential effects of dinitrates on our derived ON concentrations, and sec. 3.2.1, lines 272-273 of the revised manuscript.

Reviewer comment #6: *p. 14 VERY high Caero. So this makes your conclusions even more striking! Even at very high loading the yield was quite small.*

Author response to reviewer comment #6: The authors agree with the reviewer's comment. Under these extremely high particle mass loadings, the SOA yields are quite low, e.g., compared to β-pinene+NO_3 as shown in Fig. 2 and discussed in the revised manuscript, sec. 3.1, lines 227-229.

Reviewer comment #7: *p. 15 line 318 – could also be from RO2 + NO3.*

Author response to reviewer comment #7: Since this section refers specifically to hydroxy nitrates, the RO_2+NO_3 pathway would lead to alkoxy radical formation and NO_2. It is unclear how this pathway would lead to hydroxy nitrate formation, therefore we have not made any changes to this particular line.

Reviewer comment #7.5: *p. 15 line 365: I think there have recently been some hydroxynitrate quantifications during the FIXCIT chamber studies at Caltech, but to my knowledge none are published yet.*

Author response to reviewer comment #7.5: To our knowledge, FIXCIT was designed around measurements of isoprene oxidation products and SOA. While we have included a reference to the FIXCIT campaign in the introduction, lines 92-93 of the revised manuscript, we feel the reference is not suited for this particular section of the manuscript.

Reviewer comment #8: *p. 18 line 392: pinonaldehyde yield of 71% is not reported in Fry et al 2014. . . maybe wrong ref?*

Author response to reviewer comment #8: The yield of 71% comes from the supplementary information of *Fry et al.*, [2014]. However, since the pinonaldehyde yield was not discussed in the main text of *Fry et al.*, [2014], we have removed the reference. In addition to the pinonaldehyde yield reported in *Wangberg et al.*, [1997], we now include the *Berndt and Böge* [1997] reference in sec. 3.5, lines 473-474 of the revised manuscript, which reports a pinonaldehyde yield of 75±6%.

Reviewer comment #9: *line 394: elaborate on "similar double bond character" – because each is adjacent to a branch point?*

Author response to reviewer comment #9: The reviewer is correct that when we refer to γ-terpinene as having similar double bond character as α-pinene, we mean that both are adjacent to a branch point.

Clarification has been provided in sec. 3.5, lines 474-475 of the revised manuscript.

Reviewer comment #10: *p. 19 around lines 404-407: does the MCM produce HO2 in your simulations of the a-pinene chemistry, via the mechanism you suggest, or any other?*

Author response to reviewer comment #10: The reaction mechanism scheme, which is based on the MCM reaction scheme for α-pinene+NO_3 as described in the supplementary material, does include HO_2 as one of the byproducts of keto-nitrate formation. The mechanism also includes consumption of HO_2 and formation of the hydroperoxy nitrates by the two α- and β-nitrooxy peroxy radical isomers.

We have updated Fig. 9 (new Fig. 10), as requested in the reviewer's comment #18, to show the evolution of HO_2 based on the mechanism applied in the box model and added a discussion in sec. 3.5, lines 502-511 of the revised manuscript.

Reviewer comment #11: *p. 19, lines 415-417: Also assumes that only 1 double bond is reacted, right? Or do you include rates for each in your simple box model?*

Author response to reviewer comment #11: The *mechanism* assumes only one double bond is reacted, but the rate constant for NO_3 reaction is for that with γ-terpinene. This assumption does not affect the absolute concentration of the products. No changes have been made to the manuscript.

Reviewer comment #12: *p. 20 lines 422-425: could split out as a stacked plot to highlight the sources of NO2, whether N2O5 dissociation or decomposition?*

Author response to reviewer comment #12: We appreciate the suggestion here by the reviewer to clarify the contributions of N_2O_5 decomposition and recycling to the measured concentration of NO_2. However, since NO_2 is present in thermal equilibrium with N_2O_5 and only a small fraction is recycled following reaction (1-2%), we feel including a stacked plot doesn't add much value to Fig. 9 (new Fig. 10) or the manuscript. Besides removing the statement that the agreement between modeled and measured NO_2 concentrations in the chamber indicates reaction recycling, no other changes have been made.

Reviewer comment #13: *p. 23: is figure 1 wall-loss corrected?*

Author response to reviewer comment #13: Figure 1 was not corrected for wall loss. However, we have updated the figure to show wall loss-corrected SOA growth, consistent with our wall loss-corrected SOA yields.

Reviewer comment #14: *Fig. 2: comment on uncertainty at low Mo – looks like SOA yield is not very well constrained that low.*

Author response to reviewer comment #14: The authors agree with the reviewer. The modeled SOA yield is not very well constrained below an aerosol mass loading of ~30 μg m^{-3}. From the

95% confidence intervals, we now define the relative uncertainty in the yield at a mass loading of 10 μg m^{-3} as +100/-50%.

We have modified the text in sec. 3.1, lines 221-224 of the revised manuscript.

Reviewer comment #15: *line 491: "the right panel shows the same data on a log scale"*

Author response to reviewer comment #15: Thank you for the suggested change, we have updated the Fig. 2 description as suggested by the reviewer.

Reviewer comment #16: *Fig. 4: could be clearer if same exponent on both scales – so the number scale could be different, but as it is now, both the scale and exponent are difference which makes it hard to see the slope. Same for Fig. 5*

Author response to reviewer comment #16: Thank you for the suggested changes. Figures 4 and 5 (new Fig. 6) have been updated as suggested by the reviewer.

Reviewer comment #17: *Fig. 6: The O16 superscript in the label is a bit odd looking – necessary?*

Author response to reviewer comment #17: Thank you. It has been removed (please refer to new Fig. 8).

Reviewer comment #18: *Fig. 9: related to 2 previous comments, could show modeled HO2 here, if it produces any. And could split out NO2 into recycled vs. N2O5 dissociation sources*

Author response to reviewer comment #18: Please refer to our response to reviewer comments #10 and #12.

RESPONSES TO ANONYMOUS REVIEWER #2

The authors greatly appreciate the thoughtful critique by reviewer #2, which has greatly improved the quality of the manuscript. Below we provide a point-by-point response (shown in normal font) to the reviewer's comments (shown in italic font). The resulting additions or alterations to the manuscript are indicated in bold font and provided in an updated version of the manuscript.

Reviewer comment #1: *More discussion is needed on why no difference in yields was observed between seed and no seed experiments, particularly for the particle-phase ON yields. Current discussion (lines 253-264) is rather confusing. It is stated that under dry conditions, yields should be same with and without seed. Why? The results appear as if the yields are indistinguishable with and without seed, yet the authors state, "However, ..." (line 260). Why would hydrolysis result in different yields with and without seed? What is the particle surface area available in each experiment? What is the surface area of the wall? My concern is that much of the multifunctional ON that would readily partition to the particle-phase is getting lost on chamber walls much faster than it is adsorbing to the particle surface, and that this is the reason why no significant difference in yields are observed. Gas-phase ON loss rate due to walls was determined using the signal for C10H17NO4, which presumably would not partition to the particle-phase (or the walls) as fast as the multifunctional ON species. What is the gas-phase ON wall loss rate if C10H17NO5 was used? Perhaps it may be useful to make a figure that shows the calculated wall loss rate versus O:C or oxygen atom number or whatever for each of the major ON species shown in figure 6. The entire discussion on ON_p yields is also muddied by the statement, "...signals close to the measured background noise..." (line 258). Please clarify.*

Author response to reviewer comment #1: We greatly appreciate the reviewer's insightful comments. The insignificant difference in the particle phase ON yields between the seeded and unseeded experiments may be due to the large fraction of organic material in the particles in both cases, and for the seeded experiments, relative to sulfate. During both the seeded and unseeded experiments, particle mass increased by orders of magnitude following uptake of the oxidation products. Thus, in terms of solubility, for example, the particles are essentially the same. Without sufficient liquid water and insignificant mass fractions of hygroscopic ammonium sulfate in the particles, reactions that remove ON, such as hydrolysis, likely play an insignificant role. To clarify, sec. 3.2.2, lines 282-288 have been modified accordingly.

Wall loss of the multifunctional ON products can be a concern in the derivation of both the gas and particle phase ON yields, particularly over long experimental timescales and when the particle surface area is low relative to the surface area of the chamber walls. The effects of semi-volatile wall loss on the reported gas phase ON yields are now included in the revised manuscript, sec. 3.2.1, lines 267-272. An extended discussion of the variability in particle-phase ON yields, including the effects of wall loss, has been included in sec. 3.2.2, lines 289-298 of the revised manuscript.

Reviewer comment #2: *Rindelaub et al. (2015) found hydrolysis of ON in the particle-phase can occur at low RH. Any evidence of hydrolysis during these experiments? Possible that with seed addition, some fraction of ON was lost due to hydrolysis that would not occur without seed?*

Author response to reviewer comment #2: Thank you. Please refer to the author response given to the reviewer's initial comment. It is possible that even at the low relative humidity in our experiments, some hydrolysis, catalyzed by the presence of the hygroscopic $(NH_4)_2SO_4$ seed and particle-phase HNO_3 could aid in the removal of the nitrate functionality (Rindelaub et al., 2015b). Given the virtually indistinguishable yields between the seeded and unseeded experiments, however, we believe that hydrolysis plays a very minor role in our experiments. We have added a brief discussion of the basis of this in sec. 3.2.2, lines 298-306, from two experiments conducted with added humidity. Regardless, we have accounted for these possible effects in the uncertainty of the particle-phase ON yield as described in the text.

Reviewer comment #3: *Clarifications are needed for figure 6. What is the source of the signal between ~150 and ~320 m/z before NO3 addition? These signals do not vary with and without NO3 radical. Why? Why is there so much nitric acid in the no NO3 experiment? What is the large red signal left of the "O4" labeled peak? It is clearly enhanced by NO3. Why? Are all red signal > 320 m/z even mass? Was there no non-nitrate organic material detected with NO3 + gamma terpinene? Where is di-nitrate on this spectrum? The sum of all signal appear quite high relative to the reagent ion signal. What is iodide signal with nothing in the bag? Is the CIMS still linear with this much signal, that is, is it approaching reagent ion signal titration? Signals attributed to ON with 10 and 11 oxygen atoms highly questionable*

Author response to reviewer comment #3: The source of the peaks in Fig. 6 (new Fig. 8) between *m/z* ~150 and ~320 are associated with the background. Titration was not a concern as the reagent ion signal remained steady throughout the experiment, decreasing by ≤4% at the highest analyte concentrations. For clarity, we have updated Fig. 8 to show the relative enhancement over the background of several peaks in the presence of NO_3 and provide potential peak assignments for many of the unidentified peaks. While it is possible that the $O_{9\text{-}11}$ compounds are present in our system, we could not unambiguously make molecular assignments for them based on the mass spectra, and therefore, have removed them from Fig. 8.

Figure 6 (new Fig. 8) has been updated to reflect these changes and the discussion of this figure has been modified in sec. 3.4 lines 399-410.

Reviewer comment #4: *The discussion in the "atmospheric implication" section is inconsistent with the rest of the manuscript. These experiments were conducted near dry conditions. Discussion on mechanism focused solely on the higher volatility hydroxynitrates, not the multifunctional stuff (species with O=6, 7, 8 atoms in figure 6) that likely make up much of the ON mass in the particle-phase. Low yields all around were found. But the implication section still discusses what this may mean for SOA formation at high RH.*

Author response to reviewer comment #4: Thank you. We have added a section to the atmospheric implications regarding likely chemistry under atmospheric conditions, lines 521-523 and lines 530-536. A new figure (new Fig. 7) has been included, which reflects this chemistry.

Reviewer comment #5: *What was the relevance of ESI MS/MS to this work? Is the hydroxynitrate distinguishable from hydroperoxynitrate?*

Author response to reviewer comment #5: We appreciate the reviewer's comment as we felt we have not sufficiently highlighted the importance of our offline analysis of aerosol filter samples. While not used quantitatively, ESI MS/MS was applied to test for the presence of specific organic nitrate compounds and other oxidation products that we hypothesized were in the particle phase. This served, in part, as a means for support of the proposed mechanism shown in Fig. 8 (new Fig. 5). The hydroperoxy nitrate was distinguishable from the hydroxy nitrate based on its *m/z*. While we did not have a standard of the hydroperoxy nitrate to ensure the retention times matched that which was observed, we could, based on mass spectra and tandem mass spectra rankings, identify the chemical formula for each *m/z*.

We have provided clarification in the supplementary section.

Reviewer comment #6: *The detection of large signal that may be from a hydroperoxy nitrate is intriguing. Schwantes et al [2015 JPAa] also discussed this RO2+HO2 nighttime pathway (for isoprene). If the signal consistent with C10H17NO5 are in fact epoxides and not hydroperoxides, how would uptake differ with and without seed? What was pH of the seed particles?*

Author response to reviewer comment #6: The reviewer raises an interesting point regarding uptake of epoxides versus hydroperoxides as a function of seed and seed particle acidity. It is not entirely clear from a mechanistic standpoint how an epoxide would be produced in the gas phase from γ-terpinene oxidation by NO_3. Epoxides could, however, be produced in the condensed phase, for example, through a peroxyacyl nitrate (e.g. the corresponding PAN compound that might be produced from NO_3 reaction with terpinaldehyde), which could selectively epoxidize the remaining double bond on the hydroxy nitrate, as shown to be a very efficient epoxidation process by Darnall and Pitts (1970). Such a thermal reaction would be necessary for the dark chemistry studies here, as the isoprene epoxidation reported by Surratt et al (2010) requires OH oxidation of the precursor. Applying the Extended Aerosol Inorganics Model (E-AIM) (http://www.aim.env.uea.ac.uk/aim/aim.php), we estimate a pH ~5.5 for the $(NH_4)_2SO_4$ seed particles under saturated conditions becoming slightly more acidic as the relative humidity is decreased.

We have added a discussion in sec. 3.3, lines 354-368 of the revised manuscript regarding the pH of the particles, and the potential for condensed phase epoxidation and hydrolysis to produce species like a C10H17NO5 poly-ol, as shown in the new Fig.7.

Reviewer comment #7: *To which alpha-pinene isomers of hydroxynitrate was the iodide CIMS calibrated? Include numbers for each isomer in table. Would you expect much variability from isomer to isomer? Would you expect much variability in the sensitivity to alpha-pine derived versus gamma-terpinene derived ON?*

Author response to reviewer comment #7: We addressed this limitation in the original manuscript lines 354-363 and included the structure of the isomer in supplementary Fig. S4. The detailed synthesis and characterization of this isomer has been detailed in Rindelaub et al. (2016) and the supplementary information for that text. We have updated the text where applicable to clarify that we calibrate for only one isomer of α-pinene hydroxy nitrate.

Reviewer comment #8: *Seed particles introduced into the chamber were ~100 nm. But the particle filter had pore size 1 micron.*

Author response to reviewer comment #8: The filters were 1 μm pore size polytetrafluoroethylene (PTFE), which boasts a collection efficiency for particles between 0.01 μm and 1 μm of ~100% (Burton et al., 2007). We have updated the methods section in lines 178-176 of the revised manuscript.

Reviewer comment #9: *What was the contribution of di-nitrates to total ON? How do you account for di-nitrates with FTIR? Can FTIR distinguish mono- from di-nitrates? How does this affect the way in which ON yield is calcualted?*

Author response to reviewer comment #9: This is a good question. We did not differentiate mono- from di-nitrates using FTIR as the asymmetric -NO_2 stretch is not specific to any particular organic nitrate but all organic nitrates (Roberts, 1990). This could result in an overestimation in the reported ON yields as di-nitrates are expected to absorb more than the mono-nitrates in the wavelength region of interest. However, given the relative rate constants of alkoxy radical reaction with NO_2 (~10^{-11} cm^3 s^{-1}) and O_2 (~10^{-14} cm^3 s^{-1}) (Atkinson et al., 1982) and the relative concentrations of NO_2 (~8×10^{12} cm^{-3} maximum) and O_2 (~5×10^{18} cm^{-3}) in the chamber, we expect an insignificant contribution from first-generation di-nitrates (<0.2%). Some contribution of secondary oxidation to di-nitrates (~10%) is possible, based on the relative rates of first-generation to second-generation monoterpene oxidation.

We have updated the Methods section in lines 164-172 of the revised manuscript to address the potential influence of di-nitrates on the reported ON yields.

Reviewer comment #10: *"Teflon" (line 158) is trademark product that is similar to PTFE. So unless the filter is from Chemours that manufactures "Teflon", the appropriate description is PFA or PTFE or whatever*

Author response to reviewer comment #10: Where applicable, we have removed “Teflon” and replaced with PTFE or PFA.

RESPONSES TO ANONYMOUS REVIEWER #3

The authors greatly appreciate the careful review by reviewer #3. Below we provide a point-by-point response (shown in normal font) to the reviewer's comments (shown in italic font). The resulting additions or alterations to the manuscript are indicated in bold font in an updated version of the manuscript.

Reviewer comment #1: *The introduction is lacking sufficient references to past work and in some instances misrepresents past work. For instance, the recent review by Ng et al. (2017) should be included. Additionally, multifunctional nitrates have been identified in locations other than the Eastern US (line 84). A few (non-comprehensive) examples include Beaver et al. (2012), Rollins et al. (2013), and Yan et al. (2016).*

Author response to reviewer comment #1: Thank you. See our response to the first comment from reviewer #1. We have updated the introduction to include several other locations where multifunctional organic nitrates have been measured.

Reviewer comment #2: *Some discussion on the fate of the peroxy radical and differences/similarities in between the chamber and the atmosphere is needed. In particular, it is likely that the RO2+HO2 is under-represented in the chamber experiments. How would this influence yields and the discussion in the "atmospheric implications" section? The model based on the master chemical mechanism could help inform this question.*

Author response to reviewer comment #2: This is a good question and similar to the second comment raised by reviewer #1. For more details, please refer to the author response given to reviewer #1 and updated Fig. 9 (new Fig. 10). In short, we have updated the section on aerosol partitioning to address how differences in HO_2 between our experiments and the ambient environment affects interpretation of the SOA yield and formation of organic hydroperoxides. Moreover, Fig. 10 has been updated to show modeled HO_2 and NO_3/HO_2 ratios in the reaction chamber.

Reviewer comment #3: *The in-line reference formatting is inconsistent and do not follow the journal standards. In particular, first initials are included in the in-line references for several authors.*

Author response to reviewer comment #3: We have fixed this typo in the revised manuscript.

Reviewer comment #4: *Table 1: What is difference between the experiments on 11/12/15 and 11/18/15? They have similar deltaBVOC and ON yields but very different SOA yields. It would be useful to include the experiment length and the NO2 concentration for each experiment as well. This could help explain some of the variability seen in Figures 3-5.*

Author response to reviewer comment #4: We have updated table 1 to include the experimental time and concentration of NO_2 when it was measured. Considering the significant difference in NO_2 concentrations for these two periods, under high NO_x conditions (11/12/15 experiment), new particle formation or aerosol growth may be suppressed (lower SOA yield) due to competitive chemistry of peroxy radicals between NO_3 and HO_2, with the RO_2+NO_3 pathway leading to more

volatile reaction products. Similar observations have been made, for example, during the ozonolysis of α-pinene under high NO_x conditions (Presto et al., 2005).

We have modified the sec. 3.3 heading and provided discussion of the influence of high NO_3 concentrations and the fate of RO_2 in sec. 3.3, lines 368-375 of the revised manuscript.

Reviewer comment #5: *Figure 1: color scale missing*

Author response to reviewer comment #5: Figure 1 has been updated to include color scale.

Reviewer comment #6: *Figure 2: caption should say log scale (omit x-axis).*

Author response to reviewer comment #6: We have removed "x axis" in the caption.

Reviewer comment #7: *Figure 3/associated discussion lines 236-250: The data at deltaBVOC less than 300 ppb appears to be more scattered than the confidence interval might suggest. How much is this fit being influenced by the data points at high deltaBVOC? Or is some of the data at lower deltaBVOC influenced by more secondary oxidation? Some information on if the NO3 concentrations were similar/very different would be very helpful here.*

Author response to reviewer comment #7: Thank you for the suggestion. The reviewer is correct that the 95% confidence intervals of the fit do not capture the variability, e.g., at ΔBVOC ~ 200 ppb, and the data points above ΔBVOC ~ 300 ppb do lead to an enhancement in the yield. The exact cause of the data variability below ΔBVOC ~ 300 ppb is not entirely clear, but may be a combination of larger relative uncertainties in ΔON and ΔBVOC at lower ΔBVOC and different NO_3 concentrations and experimental timescales.

We have included a discussion of the potential causes of the variability in Fig. 3 in sec. 3.2.1, lines 264-273 of the revised manuscript.

Reviewer comment #8: *Figure 4: Please include the +2% slope as well that is stated on line 263.*

Author response to reviewer comment #8: We have modified the slopes presented in Figs. 4, 5 (new Fig. 6) and 7 (new Fig. 9), to reflect those presented in the main text.

Reviewer comment #9: *Figure 6: Please label the hydroxynitrate peak used for the yield calculation. What is the source of the peaks from m/z 200-330 that appear in both experiments? Is the large peak at m/z 190 nitric acid? If so, what is the source in the absence of NO3? Are the O9, O10, and O11 signals real? This seem difficult to identify and are difficult to interpret in the figure in the current form. This figure may benefit from a zoomed in panel of the region of interest and specific identification of the ions discussed in the manuscript.*

Author response to reviewer comment #9: Similar comments were made by reviewer #2. Please see our response to their comment #3 for more details. Briefly, the signals between *m/z* 200 and 330 are attributed to the background. We include a new trace in Fig. 6 (shown in black in new Fig. 8) that shows the enhancement over the background following addition of NO_3 to the chamber. We have removed the $O_{9\text{-}11}$ assignments as they could not be unambiguously verified. The hydroxy nitrate peak used for the yield calculation is now stated in the Fig. 8 description.

Reviewer comment #10: *Lines 75-80: I find this explanation confusing and more elaboration is needed. The NO3 oxidation of both a-pinene and b-pinene lead to tertiary peroxy radicals.*

Author response to reviewer comment #10: The authors agree with the reviewer here that this statement is too general and does not fully explain the differences in yields observed for monoterpenes that also lead to tertiary peroxy radical formation (Fry et al., 2014).

We have provided clarification in the Introduction section, lines 78-84 of the revised manuscript.

Reviewer comment #11: *Line 95: ". . .potential for ON and SOA formation are better understood." Better understood compared to what?*

Author response to reviewer comment #11: This should instead read "…better studied compared to other monoterpenes…". Lines 105-106 of the revised manuscript reflect this change.

Reviewer comment #12: *Line 133: Why not use the density of ammonium sulfate?*

Author response to reviewer comment #12: The reviewer is correct that for the seeded experiments, initial particle density should be that of $(NH_4)_2SO_4$ of ~1.7 g cm^{-3}. We have recalculated the initial seed particle mass concentration based on a density of 1.7 g cm^{-3}. Leaving the density of the SOA as 1.2 g cm^{-3} has resulted in a slight but insignificant decrease in ΔM and SOA yields for the $(NH_4)_2SO_4$ seeded experiments as presented in Table 1 and Fig. 2.

Reviewer comment #13: *Line 245-246: Wouldn't some fraction of this yield dinitrates? How is that accounted for in this calculation?*

Author response to reviewer comment #13: We have clarified this limitation in the revised manuscript as detailed in our response to comment #9 by reviewer #2.

Reviewer comment #14: *Lines 256-258: This discussion should be elaborated on and clarified. The largest amount of particulate ON measured also corresponds to some of the largest scatter which seems somewhat inconsistent with the given explanation.*

Author response to reviewer comment #14: For more details, please see comments #1 and #2 by reviewer #2 and our response to comment #7 here. In short, we have updated the discussion to include the potential influence of hydrolysis, secondary oxidation, and different RO_2 loss pathways at variable NO_3 concentrations in the chamber.

Reviewer comment #15: *Line 317: should be "nitrooxyperoxy"*

Author response to reviewer comment #15: Thank you, we have fixed this typo.

Reviewer comment #16: *Line 408-409: Since a-pinene is being used as a surrogate for g-terpinene, I assume that the assumption is that only one of the double bonds is reacting. Is this correct or is further oxidation considered?*

Author response to reviewer comment #15: The reviewer is correct, we assume that only one of the double bonds of γ-terpinene reacts with NO_3. Please refer to comment #11 by reviewer #1 for more detail.

Nitrate radical oxidation of γ-terpinene: hydroxy nitrate, total organic nitrate, and secondary organic aerosol yields

Jonathan H. Slade[1*], Chloé de Perre[2], Linda Lee[2], and Paul B. Shepson[1,3]

[1]Department of Chemistry, Purdue University, West Lafayette, IN 47907

[2]Department of Agronomy, Purdue University, West Lafayette, IN 47907

[3]Department of Earth, Atmospheric, and Planetary Sciences, Purdue University, West Lafayette, IN 47907

[*]Corresponding author: jslade@purdue.edu

Abstract

Polyolefinic monoterpenes represent a potentially important but understudied source of organic nitrates (ON) and secondary organic aerosol (SOA) following oxidation due to their high reactivity and propensity for multi-stage chemistry. Recent modeling work suggests that the oxidation of polyolefinic γ-terpinene can be the dominant source of nighttime ON in a mixed forest environment. However, the ON yields, aerosol partitioning behavior, and SOA yields from γ-terpinene oxidation by the nitrate radical (NO_3), an important nighttime oxidant, have not been determined experimentally. In this work, we present a comprehensive experimental investigation of the total (gas + particle) ON, hydroxy nitrate, and SOA yields following γ-terpinene oxidation by NO_3. Under dry conditions, the hydroxy nitrate yield = 4(+1/-3)%, total ON yield = 14(+3/-2)%, and SOA yield ≤ 10% under atmospherically-relevant particle mass loadings, similar to those for α-pinene + NO_3. Using a chemical box model, we show that the measured concentrations of NO_2 and γ-terpinene hydroxy nitrates can be reliably simulated from α-pinene + NO_3 chemistry. This suggests that NO_3 addition to either of the two internal double bonds of γ-terpinene primarily decomposes forming a relatively volatile keto–aldehyde, reconciling the small SOA yield observed here and for other internal olefinic terpenes. Based on aerosol partitioning analysis and identification of speciated particle-phase ON applying high-resolution liquid chromatography–mass spectrometry, we estimate that a significant fraction of the particle-phase ON has the hydroxy nitrate moiety. This work greatly contributes to our understanding of ON and SOA formation from polyolefin monoterpene oxidation, which could be important in the northern continental U.S. and Midwest, where polyolefinic monoterpene emissions are greatest.

1. Introduction

The oxidation of volatile organic compounds (VOCs) is a major pathway in the production of secondary organic aerosol (SOA), which can represent up to ~60% of the total submicron aerosol mass, depending on location (Hallquist et al., 2009;Riipinen et al., 2012;Glasius and Goldstein, 2016). Aerosols impact climate by scattering and absorbing radiation as well as modifying cloud optical properties, and can adversely affect human health (Stocker et al., 2013). A large fraction of the total OA budget derives from the oxidation of *biogenic* VOCs (BVOCs), including isoprene (C_5H_8) and monoterpenes ($C_{10}H_{16}$) (Hallquist et al., 2009;Spracklen et al., 2011). Together, these naturally emitted compounds account for ~60% of the global BVOC budget (Goldstein and Galbally, 2007;Guenther et al., 1995). In particular, monoterpenes, comprising ~11% of the total global BVOC emissions (Guenther, 2002), represent a viable source of SOA following oxidation (Griffin et al., 1999;Lee et al., 2006). However, atmospheric models routinely underestimate the global SOA burden (Kokkola et al., 2014), causing a potential order of magnitude error when predicting global aerosol forcing (Goldstein and Galbally, 2007), and thus the sources and mechanisms responsible for SOA formation require further study.

VOC oxidation produces an array of semi-volatile organic aerosol precursors, including organic nitrates ($RONO_2$), herein referred to as "ON", in the presence of NO_x (i.e., $NO+NO_2$) (Kroll and Seinfeld, 2008;Rollins et al., 2010b;Rollins et al., 2012;Darnall et al., 1976). By sequestering NO_x, ON can perturb ozone concentrations globally (Squire et al., 2015). Moreover, as NO_x concentrations are expected to decrease in the future (von Schneidemesser et al., 2015), ambient concentrations of NO_x and thus O_3 will become increasingly sensitive to ON formation (Tsigaridis and Kanakidou, 2007). Monoterpenes contribute significantly to the formation of ON and SOA, especially during nighttime in the presence of nitrate radicals (NO_3), when isoprene concentrations are negligible and the photolytic and NO reaction sinks of NO_3 are cut off **(see Ng**

et al. (2017) and references therein). It is estimated that monoterpene oxidation by NO_3 may account for more than half of the monoterpene-derived SOA in the U.S., suggesting that ON is a dominant SOA precursor (Pye et al., 2015). However, their formation mechanisms and yields following oxidation by NO_3 are not as well constrained as those from OH and O_3 oxidation (Hoyle et al., 2011), and previous studies have focused on the NO_3 oxidation of only a few monoterpenes (Fry et al., 2014), but almost exclusively on mono-olefinic terpenes such as α- and β-pinene (Boyd et al., 2015;Spittler et al., 2006;Wangberg et al., 1997;Fry et al., 2009;Berkemeier et al., 2016). An important detail is the relative amount of hydroxy nitrates produced, as the -OH group contributes greatly to water solubility (Shepson et al., 1996), and uptake into aqueous aerosol followed by continuing chemistry in the aqueous phase, which can be an important mechanism for SOA production (Carlton and Turpin, 2013).

A major challenge regarding our understanding of SOA formation from monoterpene oxidation is that there are several isomers of monoterpenes with very different structural characteristics that can exhibit very different yields of SOA following oxidation (Fry et al., 2014;Ziemann and Atkinson, 2012). For example, the SOA mass yield from the NO_3 oxidation of α-pinene, which contains one endocyclic double bond, is ~0% under atmospherically relevant particle mass loadings, whereas that from β-pinene, which contains one terminal double bond, is 33% under the same experimental conditions (Fry et al., 2014). Limonene, with one tertiary endo- and one terminal exocyclic double bond, also exhibits relatively larger SOA mass yields following oxidation by NO_3 (Fry et al., 2014;Spittler et al., 2006). Because NO_3 oxidation of α-pinene primarily leads to tertiary peroxy radical formation (Wangberg et al., 1997), the initially formed alkoxy radical **rearranges to a ketone and decomposes the nitrooxy group**, releasing NO_2 and forming a keto–aldehyde, which has higher saturation vapor pressure compared to its ON analogue

(Pankow and Asher, 2008). **However, decomposition of the nitrate is not exclusive for all tertiary alkoxy radicals following NO_3 oxidation as it may also depend on the structure of the adjacent bond. Based on structure–activity relationships, a β-alkyl substitution is expected to destabilize the adjacent bond more than a β-nitrate substitution (Vereecken and Peeters, 2009). In the case of β-pinene or sabinene, for example, the expected decomposition pathway of the alkoxy radical leaves the nitrooxy group intact to form a keto–nitrate (Fry et al., 2014).** SOA yields have also been shown to be strongly dependent on the total (gas + particle) yield of ON. Owing to their low saturation vapor pressures, multifunctional ON such as the hydroxy nitrates are thought to contribute significantly to SOA formation (Rollins et al., 2010a;Rollins et al., 2010b;Lee et al., 2016)**, and have been the focus of several laboratory and field research campaigns including the BEACHON 2011 field study in the Colorado front range (Fry et al., 2013), the BEARPEX 2009 study at the Blodgett forest site in the Western foothills of the Sierra Nevada (Beaver et al., 2012), the PROPHET and SOAS field studies in the upper Midwest and southeastern US (Xiong et al., 2015;Lee et al., 2016;Grossenbacher et al., 2004), and the Focused Isoprene eXperiment at the California Institute of Technology (FIXCIT) (Nguyen et al., 2014)**. These ON can **rapidly** undergo aqueous-phase processing**, especially under acid-catalyzed conditions,** to form diols and organosulfates (Jacobs et al., 2014;Rindelaub et al., 2015a;Rindelaub et al., 2016;Surratt et al., 2008), which not only **complicates quantification of organic nitrates in the aerosol phase (Russell et al., 2011), but affects product** saturation vapor pressure and thus aerosol formation, represents a sink for NO_x, and **may affect** the hygroscopic properties of organic aerosol (Suda et al., 2014). However, considering there are only a limited number of studies that have specifically investigated the yield of hydroxy nitrates, namely following OH and NO_3 oxidation of isoprene (Chen et al.,

1998;Lockwood et al., 2010;Xiong et al., 2015) and α-pinene (Rindelaub et al., 2015a;Wangberg et al., 1997), further measurements of their yields and role in aerosol formation from the oxidation of other terpenoids is critical.

In the southeastern U.S., α- and β-pinene tend to dominate monoterpene emissions (Geron et al., 2000), and their potential for ON and SOA formation are better-**studied compared to other monoterpenes** (Ayres et al., 2015;Lee et al., 2016). However, in other regions of the U.S., polyolefinic monoterpenes such as terpinene, ocimene, and limonene can be present in much greater proportions than in the southeastern US, which may be in part due to the relatively smaller abundance of the α- and β-pinene emitter southern pine, but also more polyolefinic monoterpene emitters, including *Juniperus scopulorum*, a common cedar and γ-terpinene emitter in the Midwestern US (Geron et al., 2000). In particular, model simulations suggest that the oxidation of γ-terpinene, comprising two substituted endocyclic double bonds, can contribute as much as α- and β-pinene to nighttime organic nitrate production in a mixed northern hardwood forest (Pratt et al., 2012). Those authors also showed that NO_3 reaction with BVOCs is important in the daytime. However, the ON and SOA yields following NO_3 oxidation of γ-terpinene have not been determined in laboratory studies.

Here we present a comprehensive laboratory investigation of the hydroxy nitrate, total gas and particle-phase ON, and SOA yields from the NO_3 oxidation of γ-terpinene. For the hydroxy nitrate yield experiments, a surrogate standard compound was synthesized as presented in the supplemental information of Rindelaub et al. (2016), enabling quantitative determination of its yield using a chemical ionization mass spectrometer (CIMS). This work contributes to a broader understanding of SOA formation from the oxidation of polyolefinic monoterpenes, and the role of NO_3 oxidation chemistry in the sequestration of NO_x.

2. Methods

Yield experiments were conducted in a 5500 L photochemical reaction chamber **with Teflon walls and perfluoroalkoxy (PFA)-coated endplates,** in the dark **(Chen et al., 1998)**. Briefly, the chamber was cleaned by flushing several times with ultra-zero (UZ) air in the presence of ultra-violet light. Experiments were conducted in a dry atmosphere (relative humidity < 1%) and at ambient temperature (~295 K). A total of 13 independent yield experiments were conducted over a range of initial γ-terpinene concentrations in the presence of N_2O_5 with and without $(NH_4)_2SO_4$ seed particles. N_2O_5 was produced in a dried glass vessel and crystallized at 195 K in a custom-made glass trap following thermal equilibrium with NO_2 and O_3, as indicated in reactions (1) and (2) below.

$$O_3 + NO_2 \rightarrow NO_3 + O_2 \quad (1)$$

$$NO_3 + NO_2 \leftrightarrow N_2O_5 \quad (2)$$

First, the BVOC was transferred to the chamber with UZ air via injection through a heated glass inlet and polytetrafluoroethylene (PTFE) line. For the seeded experiments, $(NH_4)_2SO_4$ particles were generated by passing an aqueous solution through a commercial atomizer (Model 3076, TSI, Inc.) and subsequently dried through a diffusion dryer prior to entering the reaction chamber. The seed particles were polydisperse with a range in the geometric mean diameter, $D_{p,g}$, of 57 nm to 94 nm and geometric standard deviation, σ_g, of 1.39 to 1.91. Total seed number and mass concentrations were in the range 0.61-5.15×10^4 cm^{-3} and 8-48 μg m^{-3}, respectively, assuming a seed particle density of **1.7 g cm^{-3}**. Yield experiments were initiated (time = 0) by injecting N_2O_5 into the chamber with a flow of UZ air over the crystalline N_2O_5. The reactants were allowed to mix continuously in the chamber with a fan, and the reaction was terminated when no less than

10% of the γ-terpinene remained to limit secondary particle-phase or heterogeneous NO_3 chemistry.

Real-time measurements were made using several instruments: γ-terpinene concentrations were measured with a gas chromatograph-flame ionization detector (GC-FID; HP-5890 Series II), which was calibrated using a commercial γ-terpinene standard dissolved in cyclohexane. NO_2 concentrations were measured with a custom-built chemiluminescence NO_x analyzer (Lockwood et al., 2010), and a scanning mobility particle sizer (SMPS; Model 3062, TSI, Inc.) was used to determine size-resolved particle mass concentrations. No direct concentration measurements of NO_3 were made. The hydroxy nitrates were measured online continuously using an iodide-adduct chemical ionization mass spectrometer (CIMS) (Xiong et al., 2015;Xiong et al., 2016). To quantify the production of monoterpene hydroxy nitrates, the CIMS was calibrated with a purified standard of an α-pinene-derived hydroxy nitrate synthesized in-house via nitrification of α-pinene oxide (Sigma–Aldrich, 97%) using $Bi(NO_3)_3 \cdot 5H_2O$ (Rindelaub et al., 2016). The concentration of the purified hydroxy nitrate was verified via two complementary methods: ^{1}HNMR and FTIR, and the structure was verified using ^{13}C-NMR, as presented in the supplementary information of Rindelaub et al. (2016). The total ON yields and concentration of the standard were determined via FTIR measurement of the asymmetric $–NO_2$ stretch located at ~1640 cm^{-1} using tetrachloroethylene (Sigma–Aldrich, HPLC grade, ≥99.9%) as the solvent (Rindelaub et al., 2015a). We n**ote that the FTIR approach cannot distinguish mono- from poly-nitrated organics. However, given the relatively low concentrations of NO_2 compared to O_2 in the chamber and their rate constants with alkoxy radicals (Atkinson et al., 1982), first-generation di-nitrates constitute an insignificant fraction of ON (<0.2%). Second-generation di-nitrates from NO_3 reaction at the remaining double bond on γ-terpinene, however, may account for a maximum of ~10% of**

the total ON based on the relative rates of primary to secondary monoterpene oxidation reactions. Thus the uncertainties for our reported yields include a component from this uncertainty (10%) in the fraction of the nitrates that are dinitrates. The total gas-phase ON yields were determined with FTIR following the sampling of chamber air through an annular denuder (URG-200) coated with XAD-4 resin and extraction from the denuder walls with tetrachloroethylene as in a previous study (Rindelaub et al., 2015a). Aerosol particles were collected on 47 mm **PTFE** filters (1 μm pore size**; ~100% collection efficiency**) housed in a cartridge connected to the denuder exit. The collection efficiency of the denuder walls for gas-phase organic nitrates was determined to be >98% based on measurements of the concentration of 2-ethyl-hexyl-nitrate (Sigma–Aldrich, 97%) before and after the denuder with the GC-FID. The particle transmission efficiency was determined to be >98% by measuring the number concentration of particles before and after the denuder with the SMPS.

Wall loss and dilution corrections were applied to both the SOA and ON yields accounting for the time required to sample through the denuder. Following several of the experiments, the SOA concentration was measured as a function of reaction time with the wall with an average wall loss rate constant, $k_{wall,SOA} = 9\times10^{-5}$ s^{-1}. The gas-phase ON wall loss rate was determined based on the evolution of the CIMS-derived monoterpene hydroxy nitrate (M=$C_{10}H_{17}NO_4$) signal ($[M+I]^-$; m/z = 342) following an experiment, in which we obtained $k_{ONg} = 2\times10^{-5}$ s^{-1}, as shown in Fig. S1.

Selected filter extracts from two separate chamber experiments were analyzed for their chemical composition via ultra-performance liquid chromatography electrospray ionization time-of-flight tandem mass spectrometry (UPLC-ESI-ToF-MS/MS, Sciex 5600+ TripleToF with Shimadzu 30 series pumps and autosampler) to identify potential ON species in the particle phase from γ-terpinene oxidation by NO_3. The samples were first dried with ultra-high purity nitrogen

and then extracted with a 1:1 v:v solvent mixture of HPLC-grade methanol and 0.1% acetic acid in nanopure H_2O, which has been used successfully as a solvent system for identifying multifunctional organonitrate and organosulfate species (Surratt et al., 2008).

3. Results and Discussion

3.1. SOA yields

Mass-dependent SOA yields (Y_{SOA}) were derived from both seeded and unseeded experiments and defined here as the change in aerosol mass concentration (ΔM in $\mu g\ m^{-3}$) relative to the concentration of BVOC consumed ($\Delta BVOC$ in $\mu g\ m^{-3}$), i.e., $Y_{SOA} = \Delta M/\Delta BVOC$. ΔM was derived from individual SOA growth curves as shown in Fig. 1. Here the initial mass is defined as the average SMPS-derived particle mass in the chamber prior to N_2O_5 injection, and the final mass is derived from the maximum of the SOA growth curve when $\Delta BVOC$ stabilizes, as shown in Fig. S2. Note that under these experimental conditions, SOA formation occurs rapidly, limited on the short end by the thermal decomposition e-folding lifetime of N_2O_5 (~30 s at 295 K) and the e-folding lifetime of NO_3 reaction with γ-terpinene (few milliseconds assuming a rate constant of 2.9×10^{-11} cm^3 $molecule^{-1}$ s^{-1}), and on the long end by the time scale for heterogeneous uptake of N_2O_5 of several hours assuming an uptake coefficient at low relative humidity of 10^{-4} (Abbatt et al., 2012).

Y_{SOA} with and without seed particles as a function of particle mass loading are depicted in Fig. 2. The curve shows that under low mass loadings, the yields are less than under high mass loadings, indicative of absorptive partitioning (Hao et al., 2011;Odum et al., 1996). To model the measured Y_{SOA} as a function of particle mass loading, we apply an absorptive partitioning model following the method of Odum et al. (1996), as shown in Eq. (1).

$$Y_{\mathrm{SOA}} = M_0 \sum_i \left(\frac{\alpha_i K_{\mathrm{om},i}}{1 + K_{\mathrm{om},i} M_0} \right)$$

Here, α_i is a proportionality constant describing the fraction of product *i* in the aerosol phase, M_0 is the aerosol mass concentration, and $K_{\mathrm{om,i}}$ is the absorptive partitioning coefficient of the absorbing material. Assuming a two-product model, the best fit values are α_1 = 0.94, $K_{\mathrm{om},1}$ = 7.9×10^{-4}, α_2 = 0.33, and $K_{\mathrm{om},1}$ = 2.6×10^{-2}. Extending this model to a conservative ambient mass loading of 10 μg m^{-3}, characteristic of biogenic SOA-impacted environments (Fry et al., 2014), the SOA yield is ~10%. **We caution that the model is not very well constrained at low mass loadings due to the limited number of data points below 30 μg m^{-3}. From the 95% confidence intervals, a conservative estimate of the relative uncertainty in the yield at 10 μg m^{-3} is +100/-50%.** In contrast, at mass loadings >500 μg m^{-3}, which is more relevant in highly polluted urban areas such as those along the coast of India (Bindu et al., 2016), Y_{SOA} can be as large as ~50%. For comparison, Y_{SOA} of other reaction systems applying the absorptive partitioning values derived from those experiments are plotted along with our experimental data in Fig. 2. The γ-terpinene + NO_3 Y_{SOA} are significantly less than those involving β-pinene, an important contributor to SOA formation predominately in the southeastern U.S (Boyd et al., 2015). However, at relatively low particle mass loadings, Y_{SOA} for NO_3 + γ-terpinene is comparable to those derived from the OH oxidation of γ-terpinene and α-pinene (Griffin et al., 1999;Lee et al., 2006). Interestingly, our measured Y_{SOA} at comparable mass loadings are also within the reported range of Y_{SOA} from the NO_3 oxidation of α-pinene of 0-16% (see Fry et al. (2014) and references therein), which are relatively small compared to other monoterpene + NO_3 reaction systems, which range from 13% to 65% for β-pinene, limonene, and Δ-3-carene **(Ng et al., 2017)**. The studies reporting low Y_{SOA} also report relatively low ON yields and high ketone yields, suggesting that the NO_3 oxidation

products of α-pinene, and likely γ-terpinene, **lose the nitrate moiety and hence** are sufficiently volatile and do not contribute significantly to SOA formation under atmospherically-relevant aerosol mass loadings. In contrast, the experiments reporting higher Y_{SOA} report relatively greater ON/ketone yield ratios, with the exception of sesquiterpenes such as β-caryophyllene, suggesting ON are important aerosol precursors.

3.2. Organic nitrate yields

ON can partition to the particle phase and contribute to SOA formation and mass growth. However, measurements of their yields are limited and highly variable depending on the composition of the reactive organic species and the type of oxidant (Ziemann and Atkinson, 2012). Here we report the measured gas- and aerosol-phase ON yields, and the total (sum of gas and aerosol ON) yield following γ-terpinene oxidation by NO_3. The ON yields (Y_{ON}) are defined as the concentration of ON produced (ΔON) either in the gas or particle phases, relative to the concentration of BVOC consumed, ΔBVOC, i.e., Y_{ON} = ΔON/ΔBVOC. In these experiments, ΔBVOC was varied systematically by altering the concentration of N_2O_5 added to the chamber and monitoring the change in BVOC concentration with the GC-FID. These experiments were conducted both in the presence and absence of $(NH_4)_2SO_4$ seed aerosol particles and under dry conditions, and corrected for wall losses and dilution.

3.2.1. Total gas-phase organic nitrate yield

As indicated in Fig. 3, the concentration of total gas-phase ON (ON_g; determined via FT-IR) increases linearly as a function of ΔBVOC, independent of the presence or absence of the seed aerosol. By fitting both the unseeded and seeded data using linear regression, we derive a gas-

phase molar ON yield (Y_{ONg}) of 11(±1)%, where the relative uncertainty in the yield of ~9% is derived from the 95% confidence intervals (shown in dashed lines in Fig. 3) of the linear fit to the data, and accounting for the measurement uncertainties, shown as error bars. The similar yields with or without seed particles implies that after some uptake, the two cases might appear identical to the adsorbing molecules. **Some of the variability in the yield presented in Fig. 3, particularly below ΔBVOC ~ 300 ppb, may be attributed to greater relative uncertainty in ΔON and ΔBVOC for low extents of BVOC reaction, different concentrations of NO_2 in the chamber, and differences in the time frame of the experiment, as indicated in Table 1. While some wall loss of the lower volatility multifunctional oxidation products could bias the reported yields low (Zhang et al., 2014), the effects of wall loss on the yield of ON are accounted for in these experiments and minimal (< 5% correction to the yield), given our relatively short experimental timescales (~40 min on average) and measured wall loss rate of the hydroxy nitrate of ~10^{-5} s^{-1}. As noted in the methods section, secondary oxidation of the remaining double bond of γ-terpinene may account for ~10% of the uncertainty in Y_{ONg}.** Regardless, Y_{ONg} observed here for γ-terpinene is considerably smaller than those measured from the NO_3 oxidation of limonene and β-pinene, but very similar to the yield from NO_3 oxidation of α-pinene (Fry et al., 2014).

3.2.2. Total particle-phase organic nitrate yield

In general, particle-phase ON concentrations (ON_p) increase with increasing ΔBVOC as shown in Fig. 4, with a particle-phase ON yield (Y_{ONp}) from the slope of 3(±1)%. Since there **were no significant differences** in ON_p **between experiments conducted** with and without seed aerosol, the slope (i.e., yield) is derived from a fit to both datasets. **The insignificant difference**

in the particle phase ON yields between the seeded and unseeded experiments may be due to the large fraction of organic material in the particles in both cases, and for the seeded experiments, relative to sulfate. During both the seeded and unseeded experiments, on average particle mass increased by orders of magnitude following uptake of the oxidation products. Thus, in terms of uptake from the gas phase, and component solubility, for example, the particles in the two cases are effectively identical. Y_{ONp} can be affected by wall loss of both semi-volatile ON products and particles. Given our relatively short experimental timescales and relatively large particle/wall surface area ratios (upwards of 0.05) compared to other studies (Nah et al., 2016;Zhang et al., 2014), wall loss corrections amount to an increase in the relative uncertainty of the yield of 8% to 39%. The greater spread in ON_p compared to ON_g (see Fig. 3) as a function of ΔBVOC may be due to variable chemistry occurring in the particle phase and the greater relative uncertainty in the case of the lower particle phase yields. It is possible that the presence of some aerosol liquid water and particle acidity, aided by the presence of hygroscopic $(NH_4)_2SO_4$ and uptake of product HNO_3 by the particles, could result in relatively lower ON_p yields, even at low relative humidity (Rindelaub et al., 2015a). However, while we did not systematically investigate the dependence of yields on hydrolysis, we did two experiments that reveal that the ONs produced here are less prone to hydrolysis. Specifically, we found that the gas (10%), particle (1%-6%), and total ON yields (11%-16%) at a relative humidity of 50% were within the uncertainty of the yields determined under dry conditions. The expected major ON product shown in the right-hand side of Fig. 5 has a secondary nitrooxy functional group, which has been shown to be less prone to hydrolysis than tertiary nitrooxy groups (Darer et al., 2011).

To account for the effects mentioned above, we estimate a more conservative aerosol organic nitrate yield of 3 (+2/-1)%, based on the upper limit of the data variability.

3.3. Organic nitrate aerosol partitioning ***and effect on SOA yield***

The sum of $ON_g + ON_p$ (ON_t) is plotted as a function of ΔBVOC in Fig. 6. Together, they result in a total molar ON yield, Y_{ONt} = 14(+3/-2)%, accounting for the potential loss of aerosol phase ON as described previously, comparable to previously measured ON yields from the NO_3 oxidation of α-pinene of 10% (Fry et al., 2014) and 14% (Wangberg et al., 1997). From the ratio Y_{ONp}/Y_{ONt}, ~20% of the total ON produced from γ-terpinene + NO_3 partitioned to the particle phase, for these relatively high aerosol mass loading conditions. Assuming an average ON molar mass of 215 g mol^{-1}, representing a C_{10}-derived hydroxy nitrate (Rindelaub et al., 2015a), roughly 14% of the total aerosol mass is comprised of ON. Gas-to-particle partitioning depends strongly on the molecule's equilibrium saturation vapor pressure and mass transfer kinetics (Shiraiwa and Seinfeld, 2012). The addition of nitrooxy and hydroxy groups, for example, can reduce the equilibrium saturation vapor pressure by several orders of magnitude (Capouet et al., 2008). Molecules with saturation vapor pressures >10^{-5} atm are almost exclusively in the gas phase, whereas those below 10^{-13} atm are almost exclusively in the condensed phase (Compernolle et al., 2011). We can estimate the saturation vapor pressure of the ON (p_i^0) based on the estimated ON aerosol mass fraction (ε_i^{aero}=0.14) as given in Eq. (2) (Valorso et al., 2011).

$$\varepsilon_i^{\mathrm{aero}} = \frac{1}{1 + \frac{M_{\mathrm{aero}} \gamma_i p_i^0}{C_{\mathrm{aero}} \mathrm{R} T}}$$

Here, M_{aero} is the average particle molar mass, γ_i is the activity coefficient of molecule "i", and C_{aero} is the aerosol mass concentration, R is the gas constant, and T is temperature. Assuming ideality, i.e., γ_i=1, $\boldsymbol{C_{aero}}$**=835 µg m^{-3}** (average of ΔM values from experiments listed in table 1), and M_{aero}=215 g mol^{-1}, we derive a p_i^0 for ON of ~6×10^{-7} atm or $\log_{10}$ saturation concentration of ~4 µg m^{-3}, which for a semivolatile C_{10}-derived hydrocarbon is expected to have between two and four oxygen atoms (Donahue et al., 2011). This estimated p_i^0 for ON is about an order of magnitude greater than that calculated for the expected tertiary hydroxy and hydroperoxy nitrates of γ-terpinene shown in Fig. 5 of 6.9×10^{-8} atm and 3.9×10^{-8} atm, respectively, using SIMPOL.1 (Pankow and Asher, 2008), suggesting that the ON_p products of γ-terpinene likely comprise a mixture of hydroperoxy and hydroxy nitrates, and other more volatile ON species, likely keto–nitrates, e.g. as shown in Fig. 5 for the case of NO_3 addition to the more-substituted carbon. For the keto–nitrate shown in Fig. 5, we calculate a p_i^0 value of 1.4×10^{-6} atm, using SIMPOL, roughly a factor of two greater than our estimate for the average for our aerosol. For comparison, the keto–aldehyde presented in Fig. 5 (γ-terpinaldehyde) has a p_i^0 value of 0.092 atm, using SIMPOL. As presented in the supplementary information, analysis of liquid extracts from filter samples using UPLC-ESI-ToF-MS/MS operated in negative ion mode indicate the presence of masses consistent with the first-generation hydroperoxy nitrate and second-generation di-hydroxy di-nitrates in the aerosol phase, the latter of which may result from both gas- and heterogeneous reactions that proceed at the unsubstituted olefinic C of a γ-terpinene hydroxy nitrate. **In the absence of substantial HO_2 in our experiments, the dominant pathway for RO_2 is likely to follow either RO_2+NO_3 or RO_2+RO_2 (when [VOC]>>N_2O_5). However, in ambient nighttime air there may be substantially more RO_2+HO_2 reactions than in our chamber experiments. Isoprene nitrooxy hydroperoxide, for example, has been identified as the major product from isoprene**

oxidation by the nitrate radical in the presence of HO_2 (Schwantes et al., 2015), and organic hydroperoxides have been identified as major SOA products from monoterpene and sesquiterpene ozonolysis (Reinnig et al., 2009;Docherty et al., 2005). Thus our chamber experiments may underestimate the concentration of hydroperoxides formed from γ-terpinene oxidation by NO_3 in the ambient environment. While we did not confirm the presence of epoxides in our experiments, and it is hard to see how an epoxide could form in the dark gas phase in these experiments, the remaining double bond of the first-generation hydroxy nitrate may be susceptible to epoxidation in the particle phase. For example, it is known that peroxyacetyl nitrate (PAN) very efficiently epoxidizes olefins in solution (Darnall and Pitts, 1970). While there would not be PAN as a product in our experiment, there could be very significant yields of the corresponding peroxy acyl nitrate from NO_3 reaction with terpinaldehyde, followed by uptake of that compound into the aerosol phase. As shown in Fig. 7 (A), that PAN compound could then react with, and produce the corresponding epoxide of any particle-phase compound with a double bond, e.g. the hydroxy nitrate, to produce a $C_{10}H_{17}O_5$ product. That epoxide would then do a pH-dependent hydrolysis in solution to produce the corresponding diol ($C_{10}H_{18}O_6$) (Jacobs et al., 2014). Applying the Extended Aerosol Inorganics Model (E-AIM) (http://www.aim.env.uea.ac.uk/aim/aim.php), we estimate a pH~5.5 for the $(NH_4)_2SO_4$ seed particles under saturated conditions, but becoming more acidic as the particles uptake HNO_3. It is important to note that the reaction products and their concentrations and thus degree of aerosol partitioning and SOA yields may also be affected by the concentration of NO_3 in the chamber. Under very high NO_x conditions as in some of the experiments here, reactions between RO_2 and NO_3 out-compete those with HO_2, which may lead to formation of relatively more volatile carbonyl reaction

products, as indicated in Fig. 5, and relative suppression of particle mass. This effect is consistent with other studies that report lower SOA yields in the presence of high NO_x concentrations (Ng et al., 2007;Presto et al., 2005;Song et al., 2005). Regardless, an aerosol mass fraction of ON of 14% is considerably less than that obtained for other monoterpenes reacting with NO_3, with the exception of α-pinene (Fry et al., 2014). This could be a result of both production of mostly volatile ON species, in particular keto–nitrates, and further reaction of the olefinic hydroxy nitrate in the aerosol phase. To verify the potential role of hydroxy nitrates in SOA production from NO_3 + γ-terpinene as well as the presence of other ON, the following section focuses on product identification of gas phase ON species using CIMS and determination of gas phase hydroxy nitrate yields.

3.4.CIMS product identification and hydroxy nitrate yields

NO_3 reactions with VOCs lead to either abstraction of a hydrogen atom or addition to a double bond. Since γ-terpinene has two double bonds with similar character, NO_3 likely has equal probability of adding to either internal double bond. However, addition of NO_3 to either one of the olefins is likely to form the more stable tertiary nitrooxy alkyl radical. Subsequent addition of O_2 forms the β-nitrooxyperoxy radical that can lead to an array of products, including hydroxy nitrates, most likely from self or cross RO_2 + RO_2 reactions or isomerization (Yeh and Ziemann, 2014;Ziemann and Atkinson, 2012). C_{10}-derived hydroxy nitrates and other multifunctional ON have been identified in field-sampled SOA particles, and for nighttime ON_p, C_{10}-derived ON could account for approximately 10% of the organic aerosol mass during the Southern Oxidant and Aerosol Study (SOAS) campaign in the U.S. southeast (Xu et al., 2015;Lee et al., 2016). However, our current understanding of C_{10}-derived hydroxy nitrate yields is limited to production via

oxidation of α-pinene (Wangberg et al., 1997). Here we expand on this by determining the hydroxy nitrate yield from γ-terpinene oxidation by NO_3 and identify other potentially important ON species using CIMS.

Figure 8 shows example CIMS mass spectra (red and blue traces) and the enhancements over the background in the presence of NO_3 (black trace) following a chamber experiment, where the enhancement is calculated from the signal for $\frac{NO_3 - no\ NO_3}{no\ NO_3}$. Several molecules were detected at masses below the iodide reagent ion signal (*m/z* = 127) following N_2O_5 addition to the chamber and correspond to NO_3^- (*m/z* = 62), $NO_3^-\cdot(H_2O)_{1,2}$ (*m/z* = 80, 98), $N_2O_5^-$ (*m/z* = 108), and what appears to be a nitrate–nitric acid cluster anion, $HN_2O_6^-$ (*m/z* = 125) (Dubowsky et al., 2015;Huey, 2007). The water cluster ions and nitric acid (also at *m/z* = 190, corresponding to $I^-\cdot HNO_3$) result from ion–molecule reactions in the humidified drift tube of our CIMS and residual HNO_3 from the N_2O_5 cold trap. Several larger molecular weight species were detected in the range of 300 ≤ *m/z* ≤ 450, consistent with products from monoterpene oxidation, with enhancements over the background as large as a factor of 50 to 100. Specifically, the first-generation hydroxy nitrates are observed at *m/z* = 342 ($C_{10}H_{17}NO_4$–I^-). Several masses follow, separated by 16 mass units, or addition of a single oxygen atom, whereby each new ON has 15, 17, or 19 H atoms. Similar observations were made in the field during the SOAS campaign for both ON_g and ON_p (Lee et al., 2016), indicating the presence of highly-functionalized ONs. It is important to note that the products observed here are derived from a single monoterpene, whereas the field ON measurements consist of products derived from all ambient monoterpene oxidation. Other major peaks included those at *m/z* = 340, potentially representing an iodide-adduct with either an aldehyde or keto–nitrate ($C_{10}H_{15}NO_4$–I^-), and *m/z* = 358, which may be indicative of an iodide-adduct with a hydroperoxy nitrate ($C_{10}H_{17}NO_5$–I^-). **A**

cluster of ions was detected above *m/z* = 400, potentially representing **molecules with higher degrees of oxygenation and secondary oxidation products such as a** di-hydroxy–di-nitrate **at *m/z* = 421** ($C_{10}H_{18}N_2O_8$–I^-), which could be formed through second-generation oxidation at the remaining unsubstituted carbon of the double bond on the first-generation hydroxy nitrate. It is important to note that the CIMS sensitivity for each of these species is likely different and depends on the polarity and acidity of the individual compound, which is affected by the type and positions of the different functional groups (Lee et al., 2016). For example, iodide-adduct CIMS is not particularly sensitive to aldehyde and carbonyl nitrates, whereas more acidic and polar molecules such as hydroxy nitrates and carboxylic acids can exhibit much greater sensitivity (Lee et al., 2016). Moreover, in general as the molecular size and number of oxygenated groups increase (particularly –OH groups), the sensitivity also increases. Hence, without commercial or custom synthetic standards, no quantitative analysis of the array of ON products could be reliably performed using this technique.

Here we determine the yield of γ-terpinene-derived hydroxy nitrates. Since there is no commercially-available standard for the expected first-generation γ-terpinene hydroxy nitrate, we use a synthetic olefinic hydroxy nitrate derived from α-pinene (structure shown in Fig. S4) for quantitative analysis (Rindelaub et al., 2016). It is possible that the CIMS is less sensitive to this nitrate compared to the more sensitive α,β-hydroxy nitrate structure expected of the first-generation γ-terpinene hydroxy nitrates, similar to the differences in the CIMS sensitivity for 4,3-isoprene hydroxy nitrate (4,3-IN) and 1,4-IN (Xiong et al., 2015). However, the use of an olefinic hydroxy nitrate is consistent with that expected from γ-terpinene oxidation because of its diolefinic character. As shown in Fig. 9, γ-terpinene-derived hydroxy nitrate concentrations increase linearly over the range of ΔBVOC with a hydroxy nitrate yield defined from the slope as 4(±1)%.

Assuming the CIMS sensitivity for the γ-terpinene hydroxy nitrates may be a factor of three greater than for our synthetic α-pinene-derived hydroxy nitrate, a more conservative estimate of the γ-terpinene-derived hydroxy nitrate yield is 4(+1/-3)%. To our knowledge, the only monoterpene hydroxy nitrate yield to have been quantified following NO_3 oxidation is 2-hydroxypinan-3-nitrate, derived from α-pinene (Wangberg et al., 1997). In that study, the hydroxy nitrate yield was determined using a combination of FT-IR and GC-ECD to be 5(±0.4)%, on the same order as the yield presented in this study for γ-terpinene using CIMS. 3-oxopinan-2-nitrate ($C_{10}H_{15}NO_4$; 213 g mol^{-1}) and a short-lived, thermally unstable peroxy nitrate ($C_{10}H_{16}N_2O_7$; 276 g mol^{-1}) were also identified in that study. It is possible that similar products are made following NO_3 oxidation of γ-terpinene, and potentially make up the signals detected at *m/z* = 340 and *m/z* = 403, respectively, as shown in Fig. 8. However, the CIMS sensitivity toward these products is expected to be relatively small compared to that for the hydroxy nitrates, due to their relatively lower polarity and acidity. Moreover, peroxy nitrates are thermally unstable and their concentrations are likely greatly reduced during transfer through the heated sampling line.

3.5.Proposed reaction mechanism

The similarities between the, at first seemingly low, γ-terpinene + NO_3-derived Y_{ONt}, hydroxy nitrate yield, and Y_{SOA} with those for NO_3 + α-pinene are provocative. This suggests the two monoterpenes may undergo very similar degradation pathways following NO_3 oxidation, which is not observed with other monoterpenes with a substituted endocyclic double bond (Fry et al., 2014). As such, our mechanistic interpretation, shown in Fig. 5, is analogous to that for the α-pinene + NO_3 reaction, as described in the Master Chemical Mechanism (MCM) (Jenkin et al., 1997;Saunders et al., 2003). NO_3 will predominately add to the C-3 (unsubstituted) position

forming the more stable tertiary alkyl radical. However, to some extent, NO_3 may also add to the second carbon forming the less stable secondary alkyl radical, approximately 35% of the time according to the MCM. Oxygen promptly adds to the alkyl radical to form either a tertiary or secondary peroxy radical (ROO·). Excess NO_2, due to thermal decomposition of N_2O_5, can add to the peroxy radical forming a thermally unstable peroxy nitrate ($-OONO_2$) in equilibrium with the peroxy radical. Subsequent RO_2· self- and cross-reactions as well as reaction with NO_3 form the alkoxy radical (RO·). The alkoxy radical can subsequently decompose to form a carbonyl nitrate or γ-terpinaldehyde (Fig. 5) and release NO_2. Analogously, pinonaldehyde is the major NO_3 oxidation product of α-pinene with reported yields of 62(±4)% (Wangberg et al., 1997) and **75±6% (Berndt and Böge, 1997)**. Given **the very similar tertiary alkoxy radicals produced from NO_3 oxidation of α-pinene and γ-terpinene, and the similar** SOA, ON_t, and hydroxy nitrate **yields, conceivably** γ-terpinaldehyde is produced and with similarly high but undetermined yields **as pinonaldehyde from α-pinene oxidation by NO_3**. Similar results have been reported for the ozonolysis of γ-terpinene, which primarily leads to decomposition and formation of γ-terpinaldehyde with a yield of 58% (Ng et al., 2006). Alternatively, disproportionation, involving a secondary peroxy radical, produces a hydroxy nitrate and a carbonyl compound from the partnering RO_2 (Yeh and Ziemann, 2014;Ziemann and Atkinson, 2012;Wangberg et al., 1997). As we have shown, the experimentally-derived yield for these products is 4%, or roughly 25% of ON_t. The remaining organic nitrate species likely contains both carbonyl and hydroperoxy (-OOH) functionalities, and perhaps peroxy nitrates, following NO_2 addition to the peroxy radical. A major species detected by our CIMS has an m/z = 358, which may represent an I^- adduct with a hydroperoxy nitrate. This product is only produced due to reactions between hydroperoxy radicals

487 (HO_2·) and RO_2· (Ziemann and Atkinson, 2012). Conceivably, HO_2· is produced in our system
488 from hydrogen abstraction from alkoxy radicals by oxygen (Wangberg et al., 1997).

489 To test the hypothesis that γ-terpinene behaves similarly to α-pinene following reaction
490 with NO_3, we ran a simple box model based on the mechanisms for NO_3 oxidation of α-pinene as
491 presented in the MCM, and compared the model output with the measured concentrations of γ-
492 terpinene, NO_2, and hydroxy nitrates. The model is constrained by the initial and final GC-FID-
493 derived concentrations of γ-terpinene. Since the nitrate radical concentration was not determined
494 experimentally, the concentration of NO_3 in the model was determined by adjusting the N_2O_5
495 concentration until the fitted concentration change of γ-terpinene matched that which was
496 measured. This approach implicitly assumes γ-terpinene is consumed only from reaction with NO_3,
497 which is expected given the orders of magnitude greater reactivity of NO_3 compared to the other
498 reactants in our system, which includes N_2O_5 and NO_2. The results of the model are presented in
499 Fig. 10. For comparison, modeled concentrations are plotted along with the measured
500 concentrations of γ-terpinene, NO_2, and hydroxy nitrates derived from one of the experiments. At
501 a first approximation, the modeled concentrations appear to be in agreement with those measured,
502 given the semi-quantitative nature of the product, particularly the hydroperoxides. **As shown in**
503 **the top panel of Fig. 10, NO_3/HO_2 ratios are ~3 at peak [HO_2], then decrease to ~1 as the**
504 **products reach steady state. In comparison, ambient nighttime NO_3/HO_2 ratios of ~1 have**
505 **been measured during the PROPHET 1998 field intensive in northern Michigan (Hurst et**
506 **al., 2001;Tan et al., 2001), and ~0.25 at the BEARPEX field site in north central California**
507 **(Bouvier-Brown et al., 2009;Mao et al., 2012). The relatively larger ratios in our chamber,**
508 **initially, suggest hydroperoxy nitrates may be underrepresented compared to the**
509 **atmosphere. Notably, the agreement between modeled and measured [NO_2] implies that**

model-derived [N_2O_5] is close to that in the reaction chamber as [NO_2] is in equilibrium with N_2O_5. Although not quantified experimentally, qualitative analysis of the CIMS mass spectra indicates the presence of carbonyl and hydroperoxy nitrates, which is consistent with the major ON products expected from the mechanism shown in Fig. 5.

4. Atmospheric Implications

The relatively low SOA and ON yields observed here under dry conditions at ambient mass loadings suggests γ-terpinene may not be an important SOA precursor at night, when NO_3 can be the dominant oxidant. However, the low saturation vapor pressure of the hydroxy nitrates, which constitute a significant portion of the total ON, and the presence of some highly oxygenated products, further suggests that these molecules are potentially important contributors to SOA mass. **While our experiments were conducted near dry conditions, in the ambient forest environment, particularly at night and in the early morning when the relative humidity near the surface is high and NO_3 reactions are competitive with O_3 and OH**, hydroxy nitrates in the particle phase can enhance SOA formation through acid-catalyzed hydrolysis and oligomerization, and in the presence of sulfates, form organic sulfates (Liu et al., 2012;Paulot et al., 2009;Rindelaub et al., 2016;Surratt et al., 2008;Rindelaub et al., 2015a), ultimately affecting the lifetime of NO_x (Browne and Cohen, 2012;Xiong et al., 2015). Furthermore, the transformation of the nitrooxy group to a hydroxyl or sulfate group will alter the hygroscopicity of the particle, making them more effective cloud condensation nuclei (Suda et al., 2014).

It is important to note that under relatively clean air conditions, the peroxy radical produced via NO_3 reaction with γ-terpinene will often react with HO_2 to produce nitrooxy hydroperoxides. As shown in the reaction scheme (B) in Fig. 7, these species can then react

with NO_3 and then HO_2, RO_2 or NO_3 again, to yield a variety of highly oxidized very low vapor pressure products that will likely partition completely to the aerosol phase. Under humid conditions, the nitrooxy groups may hydrolyze, leaving more polar/water soluble OH groups.

Although the SOA yields are low, these chamber experiments did not represent all possible reactants that can produce particle phase precursors. Recent work indicates keto–aldehydes are potentially an important source of nitrogen-containing low volatility compounds following their reaction with dimethylamine, serving as precursors to SOA and brown carbon (Duporté et al., 2016). As shown in this study, the keto–aldehyde yield is expected to be large, along with other internal olefinic terpenes. It is also important to note that the keto–aldehyde product, γ-terpinaldehyde, is olefinic. Further homogeneous and multiphase oxidation reactions at the remaining reactive double bond can potentially transform these species into oligomeric lower-volatility oxidation products, adding to the overall SOA burden (Liggio and Li, 2008). In regions such as the northern U.S., where there are greater proportions of polyolefinic monoterpenes (Geron et al., 2000), γ-terpinene may be an important reactive VOC, and thus impact aerosol and local-scale NO_x.

5. Conclusions

The total molar ON yield from the NO_3 oxidation of γ-terpinene was found to be 14(+3/-2)%. Relatively low particle-phase ON and SOA yields are consistent with previous studies that show SOA yields are generally dependent on the yield of ON. Although γ-terpinene is a diolefin, the ON, hydroxy nitrate, and SOA yields are similar to those for α-pinene oxidation by NO_3. Considering the position of the two double bonds, the expected major product is γ-terpinaldehyde,

556 which is considerably more volatile than the ON products. Box model calculations that assume
557 large keto–aldehyde yields are also in agreement with the measured concentrations of hydroxy
558 nitrates, suggesting very similar mechanistic behavior to that of α-pinene oxidation. Several gas-
559 and particle-phase ON products have been inferred from mass spectrometry analysis, indicating
560 that NO_3 reaction with γ-terpinene may be an important source of ON and dicarbonyl compounds
561 in forest-impacted environments.
562
563 **Author Contributions**
564 J. H. S. and P. B. S. designed the research and wrote the manuscript. J. H. S. performed the yield
565 experiments and analyzed the data. J. H. S. and C. d-P. analyzed the filter samples. L. L. oversaw
566 the analysis of the filter samples. All authors contributed intellectually to the manuscript.
567
568 **Acknowledgements**
569 J. H. Slade and P. B. Shepson acknowledge support from the National Science Foundation grant
570 CHE-1550398. The authors declare that they have no conflicts of interests.

Tables

Table 1. Initial conditions and yields from individual experiments. **Time indicates the period between N_2O_5 addition to the chamber and gas and particle collection by the denuder and filter. "n.m." indicates "not measured".**

Date	Seed	ΔBVOC/ ppb	ΔON_g/ ppb	ΔBVOC/ mol×10^{-4}	ΔON_p/ mol×10^{-4}	$[NO_2]$/ ppb	Time/ min	Y_{ONg}	Y_{ONp}	ΔM/ μg m^{-3}
9/9/15	None	229	10	0.52	0.012	60	52	4%	2%	530
9/17/15	None	131	16	0.30	0.025	31	30	12%	9%	272
9/19/15	None	90	7	0.20	0.017	29	28	7%	8%	311
9/21/15	None	214	15	0.48	0.007	56	73	7%	2%	604
9/23/15	None	256	21	0.58	0.017	82	18	8%	3%	534
9/23/15	None	80	8	0.18	0.007	23	31	10%	4%	61
10/20/15	$(NH_4)_2SO_4$	761	90	1.70	0.038	n.m.	62	12%	2%	3800
10/22/15	$(NH_4)_2SO_4$	164	31	0.37	0.035	n.m.	48	19%	9%	575
10/28/15	$(NH_4)_2SO_4$	47	9	0.11	0.002	7	14	18%	2%	32
11/09/15	$(NH_4)_2SO_4$	245	23	0.55	0.006	54	48	10%	1%	1143
11/10/15	$(NH_4)_2SO_4$	66	4.5	0.15	0.006	28	32	7%	4%	159
11/12/15	None	413	49	0.93	0.020	326	45	12%	2%	623
11/18/15	None	408	39	0.92	0.037	138	35	10%	4%	2206

Figures

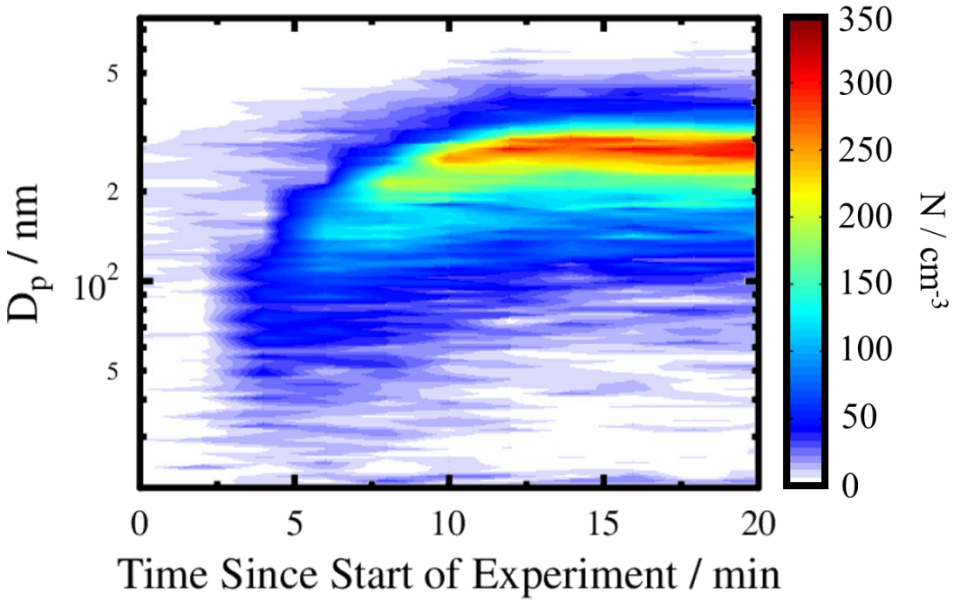

Figure 1. Example wall loss-corrected SOA growth curve for γ-terpinene + NO_3 in the absence of seed aerosol. The color scale represents aerosol number concentration, N (cm^{-3}).

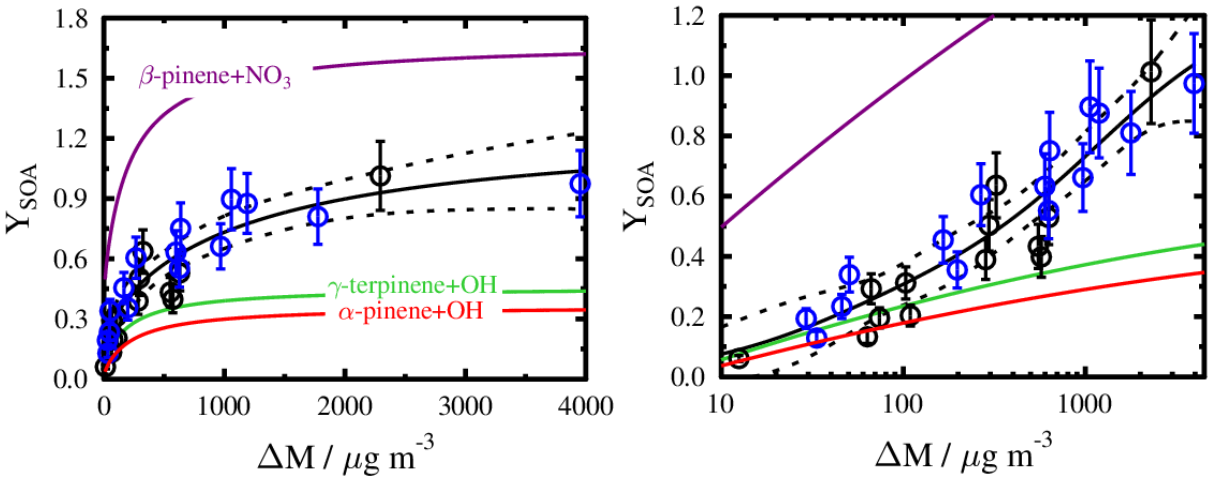

Figure 2. Change in aerosol mass concentration (ΔM) and wall-loss corrected SOA yields (Y_{SOA}) from the NO_3 oxidation of γ-terpinene in unseeded (black circles) and $(NH_4)_2SO_4$-seeded experiments (blue circles). The data were fitted to a two-product absorptive partitioning model (black curve) and the dashed curves represent the 95% confidence intervals of the fitting function. For comparison, the mass-dependent yield curves of α-pinene and γ-terpinene in the presence of OH are shown in the red and green curves, respectively, and β-pinene + NO_3 in purple (Griffin et al., 1999;Lee et al., 2006). For clarity, the right panel shows the left panel data on a log scale.

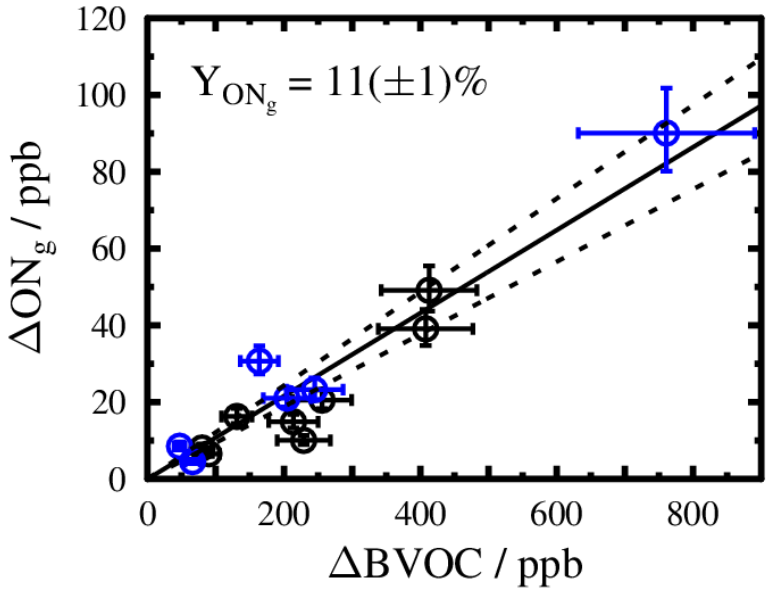

590 Figure 3. Total wall loss- and dilution-corrected gas-phase organic nitrate production (ΔON_g) as a
591 function of the amount of BVOC consumed (ΔBVOC) for the unseeded (black circles) and
592 $(NH_4)_2SO_4$-seeded experiments (blue circles). Horizontal and vertical error bars represent the
593 uncertainty in the GC-FID and FT-IR calibrations, respectively. The black line shows the linear fit
594 of the data through the origin and the dashed lines indicate the 95% confidence intervals of the fit.
595 The slopes of these lines represent the fractional organic nitrate yield and uncertainty presented in
596 the plot, respectively.

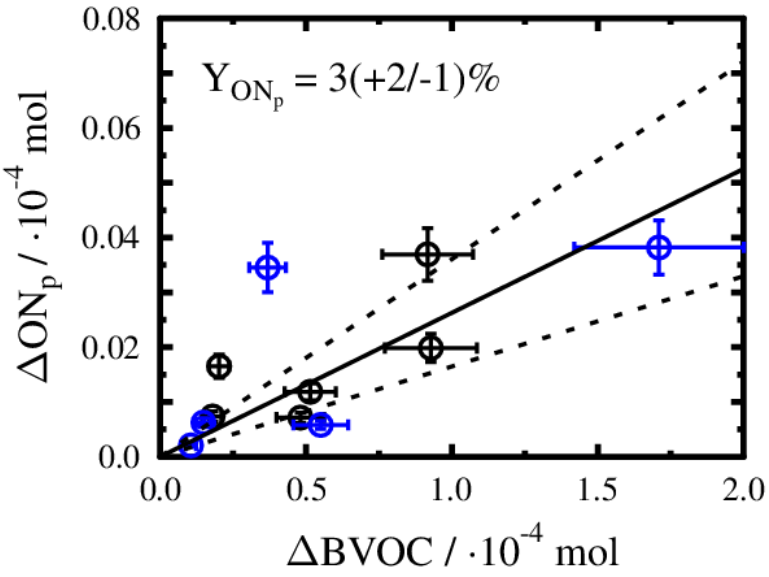

597

598 Figure 4. Total wall loss- and dilution-corrected particle-phase organic nitrate production (ΔON_p)
599 as a function of the amount of BVOC consumed (ΔBVOC) for the unseeded (black circles) and
600 $(NH_4)_2SO_4$-seeded experiments (blue circles). The **error bars and fits** are derived as in Fig. 3.

601

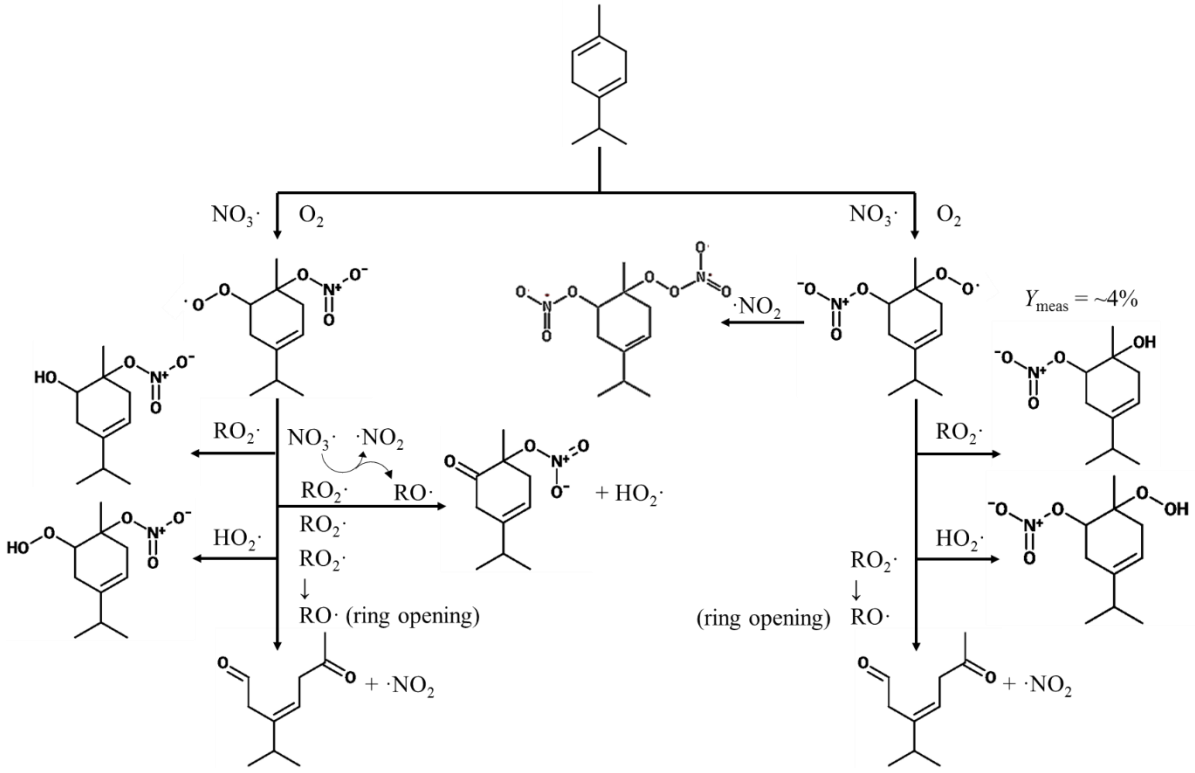

602

603 Figure 5. Proposed initial reaction pathways for the NO_3 oxidation of γ-terpinene. For simplicity,

604 only the first-generation oxidation products are shown.

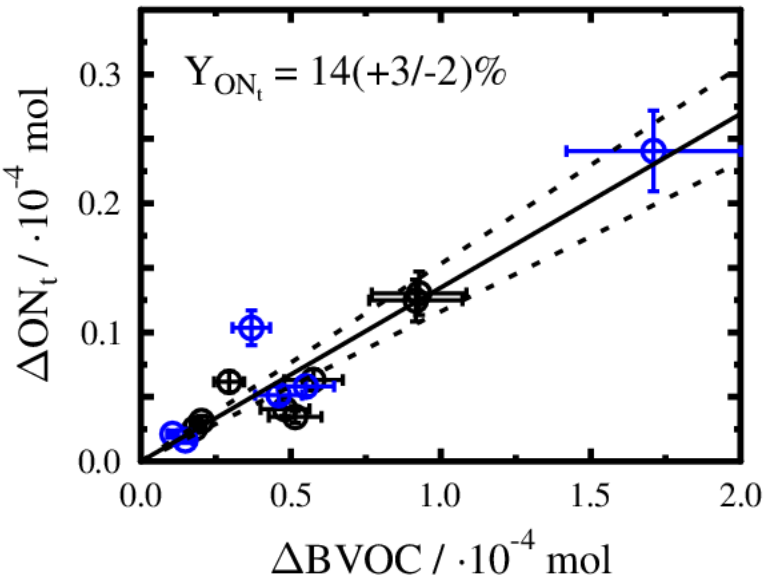

605

606 Figure 6. Total wall loss- and dilution-corrected organic nitrate production (ΔON_t) as a function
607 of the amount of BVOC consumed ($\Delta BVOC$) for the unseeded (black circles) and $(NH_4)_2SO_4$-
608 seeded experiments (blue circles). The **error bars and fits** are derived as in Fig. 3.

609

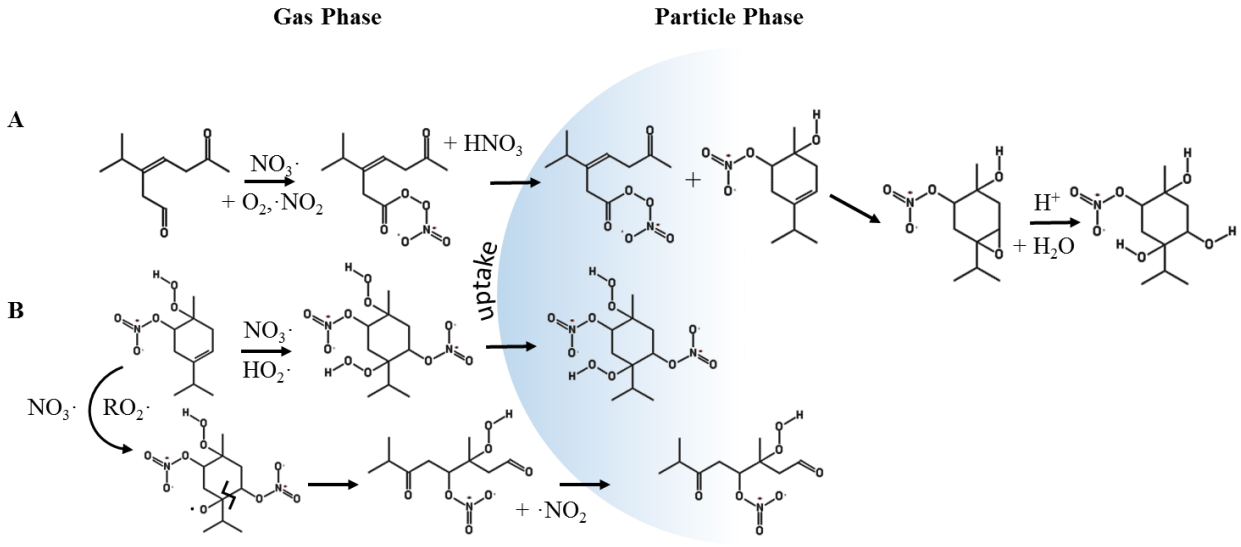

610

611 **Figure 7. Potential second-generation oxidation reactions and particle-phase chemistry. (A)**
612 **NO_3 oxidation of terpinaldehyde and olefin epoxidation by peroxy acyl nitrate, followed by**
613 **acid-catalyzed hydrolysis of the epoxide to form the diol. (B) RO_2· and HO_2· pathways**
614 **following NO_3 oxidation of the first-generation nitrooxy hydroperoxide.**

615

616

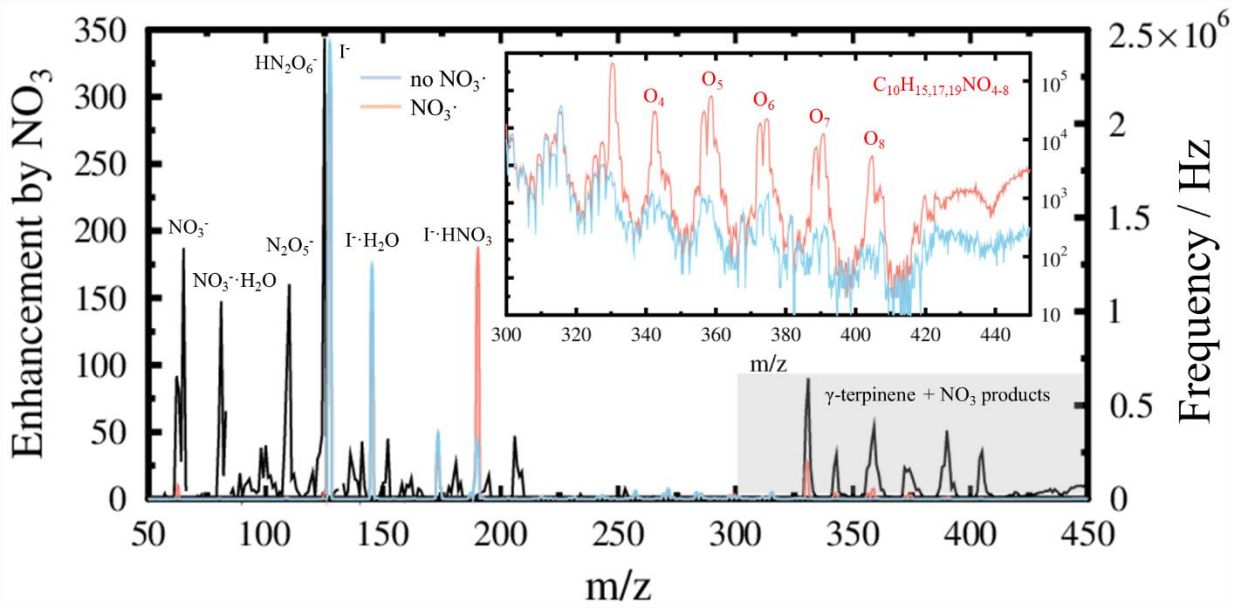

Figure 8. CIMS mass spectra before (blue) and after γ-terpinene oxidation by NO_3 (**red**) **correspond to right axis**. **Signal enhancement by addition of NO_3 is shown in the black trace.** The **inset figure shows an enhanced region of the mass spectra corresponding to the shaded area, which** indicates the presence of multifunctional ON compounds with the number of oxygen atoms consistent with the depicted chemical formula. **The "O_4" peak was used to quantify hydroxy nitrate concentrations. Signal enhancement by addition of NO_3 is shown in the black trace.**

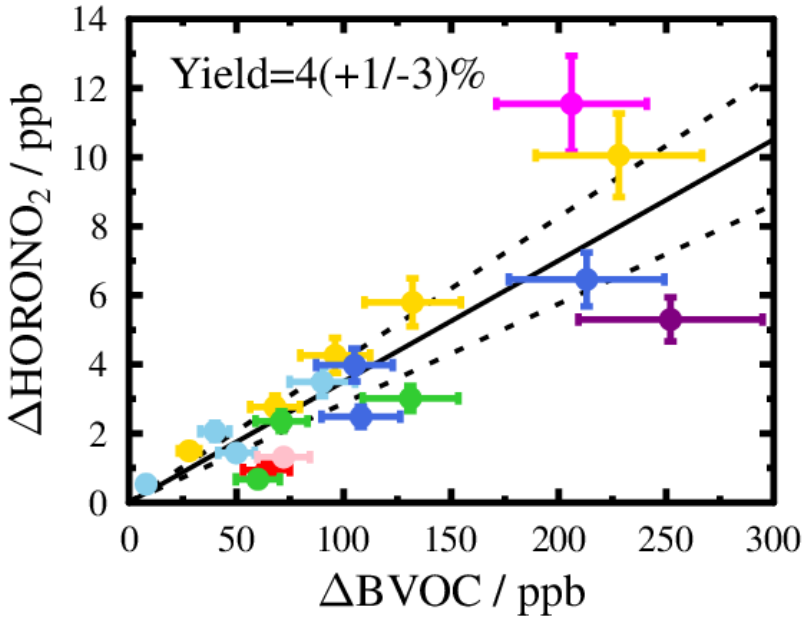

Figure 9. γ-terpinene hydroxy nitrate production ($\Delta HORONO_2$) as a function of the amount of BVOC consumed (ΔBVOC). Colors represent independent experiments performed on different days. All of the experiments were conducted in the absence of seed aerosol. The **error bars and fits** are derived as in Fig. 3.

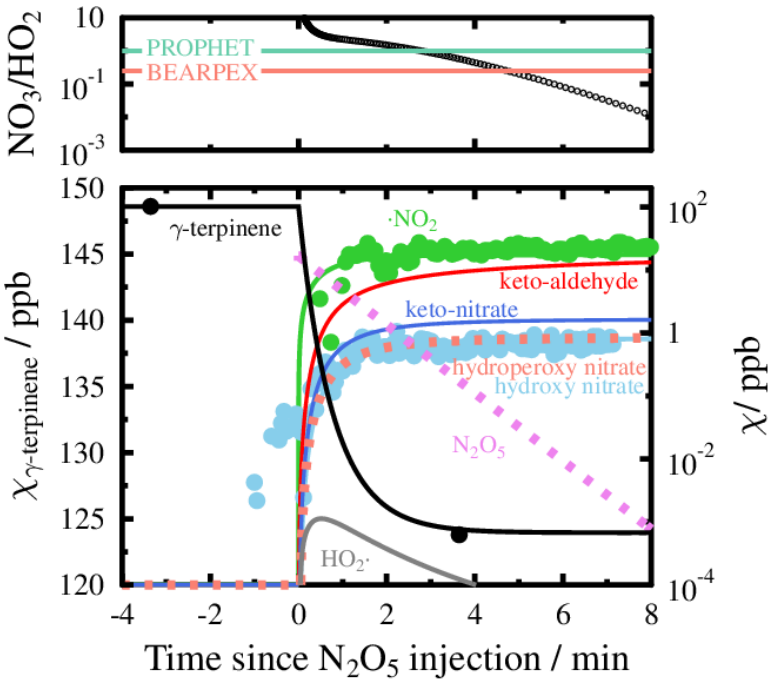

Figure 10. Time series of experiment indicating measured (circles) and modeled (lines) concentrations of γ-terpinene (black), N_2O_5 (dashed violet), NO_2 (green), HO_2 (gray), keto-aldehyde (red), keto-nitrate (dark blue), hydroperoxy nitrate (dashed pink), and hydroxy nitrate (light blue). **Top panel shows simulated NO_3/HO_2 ratios (black circles) compared to measured ambient nighttime ratios from the PROPHET and BEARPEX field intensives.** The model is based on the MCM for α-pinene reaction with NO_3.

Supplementary Information

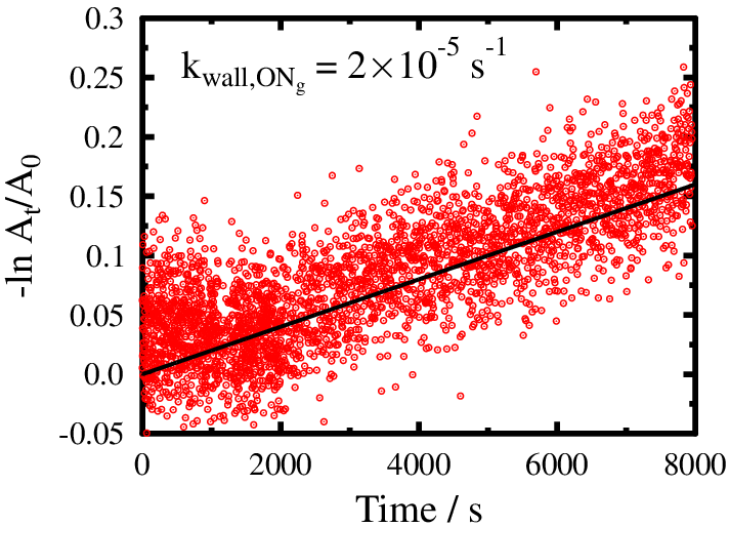

Figure S1. Wall loss rate of m/z 342 as measured by CIMS, corresponding to the monoterpene hydroxy nitrate–I^- adduct.

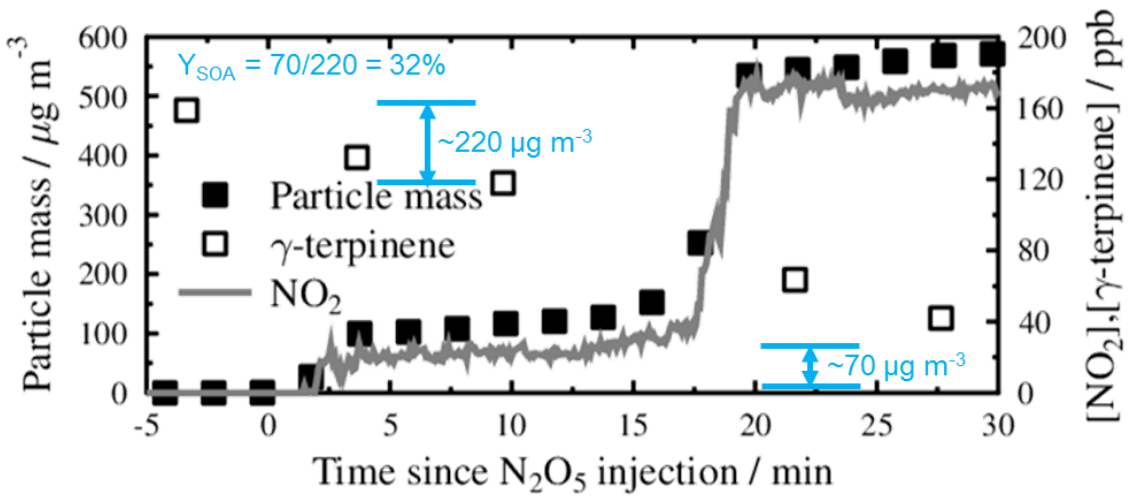

Figure S2. Example experimental time series and calculation of SOA yield.

Identification of ON in filter extracts

Figure S3 shows the extracted ion chromatograms (EIC) of the synthetic α-pinene-derived hydroxy nitrate (red), and potential particle-phase organic nitrates, including the first-generation hydroperoxy nitrate (green) and di-hydroxy di-nitrate (blue). For each EIC, there is a

652 corresponding MSMS (MS^2) spectrum, which shows the fragment ions of the parent [M+AcO^-]
653 adduct ion species. The synthesized α-pinene-derived hydroxy nitrate adduct with AcO^- (*m/z* =
654 274.1291) MS^2 spectrum indicates there are two primary fragment ions that correspond to AcO^-
655 and NO_3^-. These ions were then used as signatures to identify organic nitrate species in the filter
656 sample extracts. **Detected masses and their corresponding mass spectra and tandem mass**
657 **spectra were further analyzed and matched according to the chemical formula: $C_aH_bN_cO_d$.**
658 Of the two samples analyzed, the most abundant species with the NO_3^- fragment ion have an *m/z*
659 = 353.1197, corresponding to a molecule with chemical formula $C_{10}H_{18}N_2O_8$ + AcO^- , and *m/z* =
660 290.1241 ($C_{10}H_{17}NO_5$ + AcO^-).

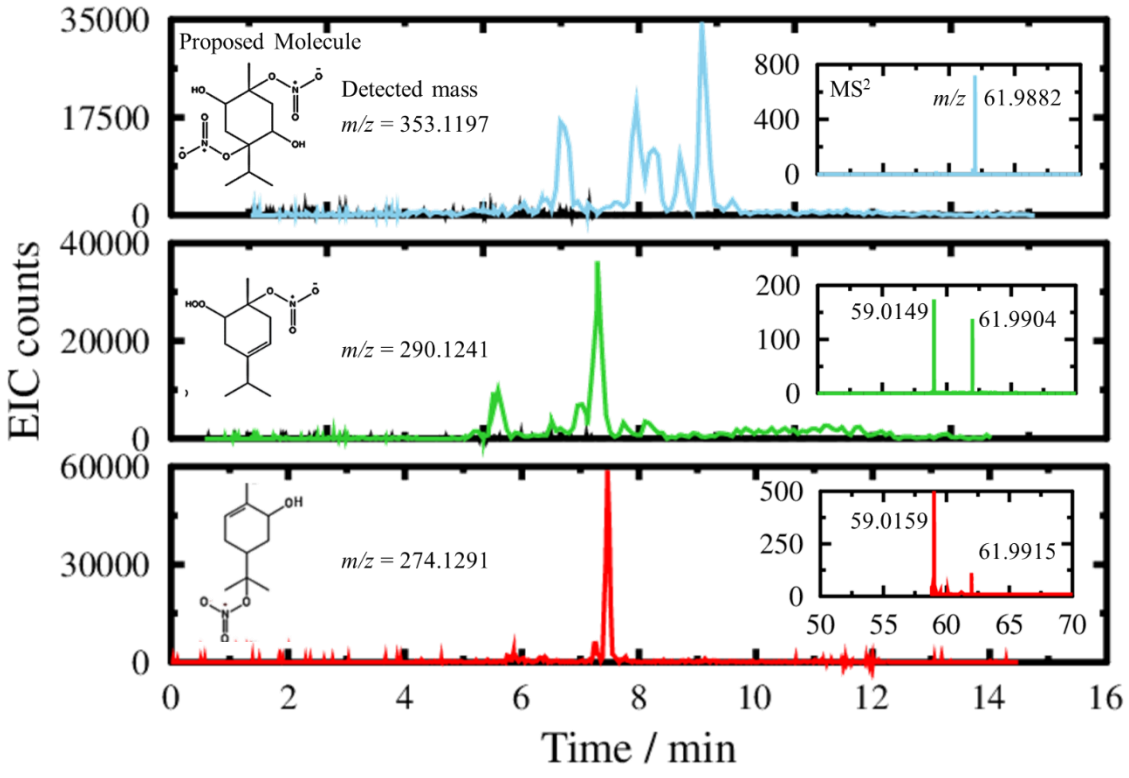

661

662 Figure S3. UPLC-ESI(-)-ToF-MS/MS extracted ion chromatograms (EIC) for the synthetic α-
663 pinene-derived hydroxy nitrate (red), hydroperoxy nitrates present in the filter extracts (green),
664 and di-hydroxy–di-nitrates present in the filter extracts (blue). For reference, the background EICs

665 (HPLC-grade methanol) for each mass are also plotted (black). The insets show the MS^2 spectra
666 and the listed *m/z* values in the MS^2 spectra correspond to the most intense peak. Potential
667 molecular structures are shown for reference.

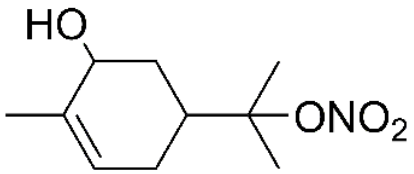

668

669 Figure S4. Molecular structure of the synthetic α-pinene-derived hydroxy nitrate used for
670 calibration of the CIMS.

671 *Box model inputs*

672 The box model applied to simulate the reaction and products from the NO_3 oxidation of γ-terpinene
673 was performed in Matlab v7.7.0 using the ordinary differential equations (ODE23s) solver in
674 Matlab. Table S1 lists the various reactions and rate constants applied in the model. The majority
675 of the rate constants were abstracted from those applied in the Master Chemical Mechanism
676 version, with the exception of NO_3 + γ-terpinene since the MCM does not explicitly include γ-
677 terpinene. Wall loss rate constants were included in the model for NO_3, N_2O_5, and the hydroxy-,
678 hydroperoxy-, and keto-nitrates as described in the footnotes of Table S1.

679 **Table S1.** Box model parameters for simulating the NO_3+γ-terpinene reaction in the chamber.

Reaction	**Rate constant**
$N_2O_5 \rightarrow NO_3 + NO_2$	$\frac{1\times10^{-12}}{2.13\times10^{-27}e^{\frac{11025}{T}}}$ cm^3 $molecule^{-1}$ s^{-1}
$NO_3 + NO_2 \rightarrow N_2O_5$	1×10^{-12} cm^3 $molecule^{-1}$ s^{-1}
[a]NO_3 + wall → loss	6×10^{-4} s^{-1}
[b]N_2O_5 + wall → loss	5×10^{-6} s^{-1}
[c]γ-terpinene + NO_3 → α-nitrooxy peroxy radical	24×10^{-12} cm^3 $molecule^{-1}$ s^{-1} *0.35

α-nitrooxy peroxy radical + NO_3 → α-nitrooxy alkoxy radical + NO_2	2.3×10^{-12} cm^3 $molecule^{-1}$ s^{-1}
α-nitrooxy peroxy radical + HO_2 → β-hydroperoxy nitrate	$2.91 \times 10^{-13} e^{\frac{1300}{T}}$ cm^3 $molecule^{-1}$ s^{-1} *0.914
α-nitrooxy peroxy radical + RO_2 → β-hydroxy nitrate	2.5×10^{-13} cm^3 $molecule^{-1}$ s^{-1} *0.1
α-nitrooxy peroxy radical + RO_2 → α-nitrooxy alkoxy radical	2.5×10^{-13} cm^3 $molecule^{-1}$ s^{-1} *0.8
α-nitrooxy peroxy radical + RO_2 → β-keto nitrate	2.5×10^{-13} cm^3 $molecule^{-1}$ s^{-1} *0.1
α-nitrooxy alkoxy radical + O_2 → β-keto nitrate + HO_2	$2.5 \times 10^{-14} e^{\frac{-300}{T}}$ cm^3 $molecule^{-1}$ s^{-1}
α-nitrooxy-β-alkoxy radical → keto-aldehyde + NO_2	4×10^{5} s^{-1}
[c]γ-terpinene + NO_3 → β-nitrooxy peroxy radical	24×10^{-12} cm^3 $molecule^{-1}$ s^{-1} *0.65
β-nitrooxy peroxy radical + NO_3 → β-nitrooxy alkoxy radical + NO_2	2.3×10^{-12} cm^3 $molecule^{-1}$ s^{-1}
β-nitrooxy peroxy radical + HO_2 → α-hydroperoxy nitrate	$2.91 \times 10^{-13} e^{\frac{1300}{T}}$ cm^3 $molecule^{-1}$ s^{-1} *0.914
β-nitrooxy peroxy radical + RO_2 → α-hydroxy nitrate	6.7×10^{-15} cm^3 $molecule^{-1}$ s^{-1} *0.1
β-nitrooxy peroxy radical + RO_2 → β-nitrooxy alkoxy radical	6.7×10^{-15} cm^3 $molecule^{-1}$ s^{-1} *0.9
β-nitrooxy alkoxy radical → keto-aldehyde + NO_2	1×10^{6} s^{-1}
[d]Wall loss rate of hydroxy nitrate, keto nitrate, and hydroperoxy nitrate	2×10^{-5} s^{-1}

[a]Wall loss rate from Fry et al. (2009). [b]Wall loss rate from Perring et al. (2009). [c]Reaction rate constant from Martinez et al. (1999). [d]Wall loss rates derived from the measurement of hydroxy nitrate wall loss.

683 **References**

684 Abbatt, J. P. D., Lee, A. K. Y., and Thornton, J. A.: Quantifying trace gas uptake to tropospheric
685 aerosol: recent advances and remaining challenges, Chem. Soc. Rev., 41, 6555-6581,
686 10.1039/C2cs35052a, 2012.

687 Atkinson, R., Aschmann, S. M., Carter, W. P. L., Winer, A. M., and Pitts, J. N.: Alkyl Nitrate
688 Formation from the Nox-Air Photooxidations of C2-C8 N-Alkanes, J. Phys. Chem., 86, 4563-
689 4569, DOI 10.1021/j100220a022, 1982.

690 Ayres, B. R., Allen, H. M., Draper, D. C., Brown, S. S., Wild, R. J., Jimenez, J. L., Day, D. A.,
691 Campuzano-Jost, P., Hu, W., de Gouw, J., Koss, A., Cohen, R. C., Duffey, K. C., Romer, P.,
692 Baumann, K., Edgerton, E. S., Takahama, S., Thornton, J. A., Lee, B. H., Lopez-Hilfiker, F., Mohr,
693 C., Wennberg, P. O., Nguyen, T. B., Teng, A. P., Goldstein, A. H., Olson, K., and Fry, J. L.:
694 Organic nitrate aerosol formation via NO_3 + biogenic volatile organic compounds in the
695 southeastern United States, Atmos. Chem. Phys., 15, 13377-13392, 10.5194/acp-15-13377-2015,
696 2015.

697 Beaver, M. R., St. Clair, J. M., Paulot, F., Spencer, K. M., Crounse, J. D., LaFranchi, B. W., Min,
698 K. E., Pusede, S. E., Wooldridge, P. J., Schade, G. W., Park, C., Cohen, R. C., and Wennberg, P.
699 O.: Importance of biogenic precursors to the budget of organic nitrates: observations of
700 multifunctional organic nitrates by CIMS and TD-LIF during BEARPEX 2009, Atmos. Chem.
701 Phys., 12, 5773-5785, 10.5194/acp-12-5773-2012, 2012.

702 Berkemeier, T., Ammann, M., Mentel, T. F., Pöschl, U., and Shiraiwa, M.: Organic nitrate
703 contribution to new particle formation and growth in secondary organic aerosols from alpha-
704 pinene ozonolysis, Environ. Sci. Technol., 50, 6334-6342, 10.1021/acs.est.6b00961, 2016.

705 Berndt, T., and Böge, O.: Products and mechanisms of the gas-phase reaction of NO_3 radicals with
706 α-pinene, J. Chem. Soc. Fraday Trans., 93, 3021-3027, 10.1039/a702364b, 1997.

707 Bindu, G., Nair, P. R., Aryasree, S., Hegde, P., and Jacob, S.: Pattern of aerosol mass loading and
708 chemical composition over the atmospheric environment of an urban coastal station, J. Atmos.
709 Sol-Terr. Phy., 138-139, 121-135, 10.1016/j.jastp.2016.01.004, 2016.

710 Bouvier-Brown, N. C., Goldstein, A. H., Gilman, J. B., Kuster, W. C., and de Gouw, J. A.: In-situ
711 ambient quantification of monoterpenes, sesquiterpenes, and related oxygenated compounds
712 during BEARPEX 2007: implications for gas- and particle-phase chemistry, Atmos. Chem. Phys.,
713 9, 5505-5518, 2009.

714 Boyd, C. M., Sanchez, J., Xu, L., Eugene, A. J., Nah, T., Tuet, W. Y., Guzman, M. I., and Ng, N.
715 L.: Secondary organic aerosol formation from the beta-pinene + NO3 system: effect of humidity
716 and peroxy radical fate, Atmos. Chem. Phys., 15, 7497-7522, 10.5194/acp-15-7497-2015, 2015.

717 Browne, E. C., and Cohen, R. C.: Effects of biogenic nitrate chemistry on the NO_x lifetime in
718 remote continental regions, Atmos. Chem. Phys., 12, 11917-11932, 10.5194/acp-12-11916-2012,
719 2012.

Burton, N. C., Grinshpun, S. A., and Reponen, T.: Physical collection efficiency of filter materials for bacteria and viruses, Ann. Occup. Hyg., 51, 143-151, 10.1093/annhyg/mel073, 2007.

Capouet, M., Müller, J.-F., Ceulemans, K., Compernolle, S., and Vereecken, L.: Modeling aerosol formation in alpha-pinene photo-oxidation experiments, J. Geophys. Res., 113, 10.1029/2007JD008995, 2008.

Carlton, A. G., and Turpin, B. J.: Particle partitioning potential of organic compounds is highest in the Eastern US and driven by anthropogenic water, Atmos. Chem. Phys., 13, 10203-10214, 10.5194/acp-13-10203-2013, 2013.

Chen, X., Hulbert, D., and Shepson, P. B.: Measurement of the organic nitrate yield from OH reaction with isoprene, J. Geophys. Res., 103, 25563-25568, 10.1029/98JD01483, 1998.

Compernolle, S., Ceulemans, K., and Müller, J.-F.: EVAPORATION: a new vapour pressure estimation method for organic molecules including non-additivity and intramolecular interactions, Atmos. Chem. Phys., 11, 9431-9450, 10.5194/acp-11-9431-2011, 2011.

Darer, A. I., Cole-Filipiak, N. C., O'Connor, A. E., and Elrod, M. J.: Formation and stability of atmospherically relevant isoprene-derived organosulfates and organonitrates, Environ. Sci. Technol., 45, 1895-1902, 10.1021/es103797z, 2011.

Darnall, K. R., and Pitts, J. N.: Peroxyacetyl Nitrate - a Novel Reagent for Oxidation of Organic Compounds, J Chem Soc Chem Comm, 1305-&, DOI 10.1039/c29700001305, 1970.

Darnall, K. R., Carter, W. P. L., Winer, A. M., Lloyd, A. C., and Pitts, J. N.: Importance of RO2+NO in alkyl nitrate formation from C4-C6 alkane photooxidations under simulated atmospheric conditions, J. Phys. Chem., 80, 1948-1950, 10.1021/j100558a029, 1976.

Docherty, K. S., Wu, W., Lim, Y. B., and Ziemann, P. J.: Contributions of organic peroxides to secondary aerosol formed from reactions of monoterpenes with O-3, Environ. Sci. Technol., 39, 4049-4059, 10.1021/es050228s, 2005.

Donahue, N. M., Epstein, S. A., Pandis, S. N., and Robinson, A. L.: A two-dimensional volatility basis set: 1. organic-aerosol mixing thermodynamics, Atmos. Chem. Phys., 11, 3308-3318, 10.5194/acp-11-3303-2011, 2011.

Dubowsky, S. E., Friday, D. M., Peters, K. C., Zhao, Z. J., Perry, R. H., and McCall, B. J.: Mass spectrometry of atmospheric-pressure ball plasmoids, Int. J. Mass Spectrom., 376, 39-45, 10.1016/j.ijms.2014.11.011, 2015.

Duporté, G., Parshintsev, J., Barreira, L. M. F., Hartonen, K., Kulmala, M., and Riekkola, M. L.: Nitrogen-containing low volatile compounds from pinonaldehyde-dimethylamine reaction in the atmosphere: a laboratory and field study, Environ. Sci. Technol., 50, 4693-4700, 10.1021/acs.est.6b00270, 2016.

Fry, J. L., Kiendler-Scharr, A., Rollins, A. W., Wooldridge, P. J., Brown, S. S., Fuchs, H., Dube, W., Mensah, A., dal Maso, M., Tillmann, R., Dorn, H. P., Brauers, T., and Cohen, R. C.: Organic

nitrate and secondary organic aerosol yield from NO_3 oxidation of beta-pinene evaluated using a gas-phase kinetics/aerosol partitioning model, Atmos. Chem. Phys., 9, 1431-1449, 10.5194/acp-9-2009-1431-1449, 2009.

Fry, J. L., Draper, D. C., Zarzana, K. J., Campuzano-Jost, P., Day, D. A., Jimenez, J. L., Brown, S. S., Cohen, R. C., Kaser, L., Hansel, A., Cappellin, L., Karl, T., Hodzic Roux, A., Turnipseed, A., Cantrell, C., Lefer, B. L., and Grossberg, N.: Observations of gas- and aerosol-phase organic nitrates at BEACHON-RoMBAS 2011, Atmos. Chem. Phys., 13, 8585-8605, 10.5194/acp-13-8585-2013, 2013.

Fry, J. L., Draper, D. C., Barsanti, K. C., Smith, J. N., Ortega, J., Winkler, P. M., Lawler, M. J., Brown, S. S., Edwards, P. M., Cohen, R. C., and Lee, L.: Secondary organic aerosol formation and organic nitrate yield from NO_3 oxidation of biogenic hydrocarbons, Environ. Sci. Technol., 48, 11944-11953, 10.1021/es502204x, 2014.

Geron, C., Rasmussen, R., Arnts, R., and Guenther, A. B.: A review and synthesis of monoterpene speciation from forests in the United States, Atmos. Environ., 34, 1761-1781, 10.1016/S1352-2310(99)00364-7, 2000.

Glasius, M., and Goldstein, A. H.: Recent discoveries and future challenges in atmospheric organic chemistry, Environ. Sci. Technol., 50, 2754-2764, 10.1021/acs.est.5b05105, 2016.

Goldstein, A. H., and Galbally, I. E.: Known and unexplored organic constituents in the Earth's atmosphere, Environ. Sci. Technol., 41, 1514-1521, 10.1021/es072476p, 2007.

Griffin, R. J., Cocker III, D. R., Flagan, R. C., and Seinfeld, J. H.: Organic aerosol formation from the oxidation of biogenic hydrocarbons, J. Geophys. Res., 104, 3555-3567, 10.1029/1998JD100049, 1999.

Grossenbacher, J. W., Barket, D. J., Shepson, P. B., Carroll, M. A., Olszyna, K., and Apel, E.: A comparison of isoprene nitrate concentrations at two forest-impacted sites, J. Geophys. Res.-Atmos., 109, 10.1029/2003jd003966, 2004.

Guenther, A., Hewitt, C. N., Erickson, D., Fall, R., Geron, C., Graedel, T., Harley, P., Klinger, L., Lerdau, M., Mckay, W. A., Pierce, T., Scholes, B., Steinbrecher, R., Tallamraju, R., Taylor, J., and Zimmerman, P.: A global model of natural volatile organic compound emissions, J. Geophys. Res., 100, 8873-8892, 10.1029/94JD02950, 1995.

Guenther, A.: The contribution of reactive carbon emissions from vegetation to the carbon balance of terrestrial ecosystems, Chemosphere, 49, 837-844, 10.1016/S0045-6535(02)00384-3, 2002.

Hallquist, M., Wenger, J. C., Baltensperger, U., Rudich, Y., Simpson, D., Claeys, M., Dommen, J., Donahue, N. M., George, C., Goldstein, A. H., and Hamilton, J. F.: The formation, properties and impact of secondary organic aerosol: current and emerging issues, Atmos. Chem. Phys., 9, 5155-5236, 10.5194/acp-9-5155-2009, 2009.

Hao, L. Q., Romakkaniemi, S., Yli-Pirila, P., Joutsensaari, J., Kortelainen, A., Kroll, J. H., Miettinen, P., Vaattovaara, P., Tiitta, P., Jaatinen, A., Kajos, M. K., Holopainen, J. K., Heijari, J.,

793 Rinne, J., Kulmala, M., Worsnop, D. R., Smith, J. N., and Laaksonen, A.: Mass yields of secondary
794 organic aerosols from the oxidation of alpha-pinene and real plant emissions, Atmos. Chem. Phys.,
795 11, 1367-1378, 10.5194/acp-11-1367-2011, 2011.

796 Hoyle, C. R., Boy, M., Donahue, N. M., Fry, J. L., Glasium, M., Guenther, A., Hallar, A. G., Huff
797 Hartz, K., Petters, M. D., Petaja, T., Rosenoern, T., and Sullivan, A. P.: A review of the
798 anthropogenic influence on biogenic secondary organic aerosol, Atmos. Chem. Phys., 11, 321-
799 343, 10.5194/acp-11-321-2011, 2011.

800 Huey, L. G.: Measurement of trace atmospheric species by chemical ionization mass spectrometry:
801 Speciation of reactive nitrogen and future directions, Mass Spectrom. Rev., 26, 166-184,
802 10.1002/mas.20118, 2007.

803 Hurst, J. M., Barket, D. J., Herrera-Gomez, O., Couch, T. L., Shepson, P. B., Faloona, I., Tan, D.,
804 Brune, W., Westberg, H., Lamb, B., Biesenthal, T., Young, V., Goldstein, A., Munger, J. W.,
805 Thornberry, T., and Carroll, M. A.: Investigation of the nighttime decay of isoprene, J. Geophys.
806 Res.-Atmos., 106, 24335-24346, Doi 10.1029/2000jd900727, 2001.

807 Jacobs, M. I., Burke, W. J., and Elrod, M. J.: Kinetics of the reactions of isoprene-derived
808 hydroxynitrates: gas phase epoxide formation and solution phase hydrolysis, Atmos. Chem. Phys.,
809 14, 8933-8946, 10.5194/acp-14-8933-2014, 2014.

810 Jenkin, M. E., Saunders, S. M., and Pilling, M. J.: The tropospheric degradation of volatile organic
811 compounds: A protocol for mechanism development, Atmos. Environ., 31, 81-104,
812 10.1016/S1352-2310(96)00105-7, 1997.

813 Kokkola, H., Yli-Pirila, P., Vesterinen, M., Korhonen, H., Keskinen, H., Romakkaniemi, S., Hao,
814 L., Kortelainen, A., Joutsensaari, J., Worsnop, D. R., Virtanen, A., and Lehtinen, K. E. J.: The role
815 o flow volatile organics on secondary organic aerosol formation, Atmos. Chem. Phys., 14, 1689-
816 1700, 10.5194/acp-14-1689-2014, 2014.

817 Kroll, J. H., and Seinfeld, J. H.: Chemistry of secondary organic aerosol: formation and evolution
818 of low-volatility organics in the atmosphere, Atmos. Environ., 42, 3593-3624,
819 10.1016/j.atmosenv.2008.01.003, 2008.

820 Lee, A., Goldstein, A. H., Kroll, J. H., Ng, N. L., Varutbangkul, V., Flagan, R. C., and Seinfeld, J.
821 H.: Gas-phase products and secondary aerosol yields from the photooxidation of 16 different
822 terpenes, J. Geophys. Res., 111, D17305, 10.1029/2006JD007050, 2006.

823 Lee, B. H., Mohr, C., Lopez-Hilfiker, F. D., Lutz, A., Hallquist, M., Lee, L., Romer, P., Cohen, R.
824 C., Lyer, S., Kurten, T., Hu, W., Day, D. A., Campuzano-Jost, P., Jimenez, J. L., Xu, L., Ng, N.
825 L., Guo, H., Weber, R. J., Wilde, R. J., Brown, S. S., Koss, A., de Gouw, J., Olson, K., Goldstein,
826 A. H., Seco, R., Kim, S., McAvey, K. M., Shepson, P. B., Starn, T. K., Baumann, K., Edgerton,
827 E. S., Liu, J., Shilling, J. E., Miller, D. O., Brune, W., Schobesberger, S., D'Ambro, E. L., and
828 Thornton, J. A.: Highly functionalized organic nitrates in the southeast United States: contribution
829 to secondary organic aerosol and reactive nitrogen budgets, Proc. Nat. Acad. Sci., 113, 1516-1521,
830 10.1073/pnas.1508108113, 2016.

Liggio, J., and Li, S.-M.: Reversible and irreversible processing of biogenic olefins on acidic aerosols, Atmos. Chem. Phys., 8, 2039-2055, 10.5194/acp-8-2039-2008, 2008.

Liu, S., Shilling, J. E., Song, C., Hiranuma, N., Zaveri, R. A., and Russell, L. M.: Hydrolysis of organonitrate functional groups in aerosol particles, Aerosol Sci. Technol., 46, 1359-1369, 10.1080/02786826.2012.716175, 2012.

Lockwood, A. L., Shepson, P. B., Fiddler, M. N., and Alaghmand, M.: Isoprene nitrates: preparation, separation, identification, yields, and atmospheric chemistry, Atmos. Chem. Phys., 10, 6169-6178, 10.5194/acp-10-6169-2010, 2010.

Mao, J., Ren, X., Zhang, L., Van Duin, D. M., Cohen, R. C., Park, J. H., Goldstein, A. H., Paulot, F., Beaver, M. R., Crounse, J. D., Wennberg, P. O., DiGangi, J. P., Henry, S. B., Keutsch, F. N., Park, C., Schade, G. W., Wolfe, G. M., Thornton, J. A., and Brune, W. H.: Insights into hydroxyl measurements and atmospheric oxidation in a California forest, Atmos. Chem. Phys., 12, 8009-8020, 10.5194/acp-12-8009-2012, 2012.

Martinez, E., Cabañas, B., Aranda, A., Martin, P., and Salgado, S.: Absolute rate coefficients for the gas-phase reactions of NO_3 radical with a series of monoterpenes at T=298 to 433 K, J. Atmos. Chem., 33, 265-282, 10.1023/A:1006178530211, 1999.

Nah, T., Mcvay, R. C., Zhang, X., Boyd, C. M., Seinfeld, J. H., and Ng, N. L.: Influence of seed aerosol surface area and oxidation rate on vapor wall deposition and SOA mass yields: a case study with alpha-pinene ozonolysis, Atmos. Chem. Phys., 16, 9361-9379, 10.5194/acp-16-9361-2016, 2016.

Ng, N. L., Kroll, J. H., Keywood, M. D., Bahreini, R., Varutbangkul, V., Flagan, R. C., Seinfeld, J. H., Lee, A., and Goldstein, A. H.: Contribution of first- versus second-generation products to secondary organic aerosols formed in the oxidation of biogenic hydrocarbons, Environ. Sci. Technol., 40, 2283-2297, 10.1021/es052269u, 2006.

Ng, N. L., Chhabra, P. S., Chan, A. W. H., Surratt, J. D., Kroll, J. H., Kwan, A. J., McCabe, D. C., Wennberg, P. O., Sorooshian, A., Murphy, S. M., Dalleska, N. F., Flagan, R. C., and Seinfeld, J. H.: Effect of NO_x level on secondary organic aerosol (SOA) formation from the photooxidation of terpenes, Atmos. Chem. Phys., 7, 5159-5174, 10.5194/acp-7-5159-2007, 2007.

Ng, N. L., Brown, S. S., Archibald, A. T., Atlas, E., Cohen, R. C., Crowley, J. N., Day, D. A., Donahue, N. M., Fry, J. L., Fuchs, H., Griffin, R. J., Guzman, M. I., Herrmann, H., Hodzic, A., Iinuma, Y., Jimenez, J. L., Kiendler-Scharr, A., Lee, B. H., Luecken, D. J., Mao, J., McLaren, R., Mutzel, A., Osthoff, H. D., Ouyang, B., Picquet-Varrault, B., Platt, U., Pye, H. O. T., Rudich, Y., Schwantes, R. H., Shiraiwa, M., Stutz, J., Thornton, J. A., Tilgner, A., Williams, B. J., and Zaveri, R. A.: Nitrate radicals and biogenic volatile organic compounds: oxidation, mechanisms, and organic aerosol, Atmos. Chem. Phys., 17, 2103-2162, 10.5194/acp-17-2103-2017, 2017.

Nguyen, T. B., Crounse, J. D., Schwantes, R. H., Teng, A. P., Bates, K. H., Zhang, X., St. Clair, J. M., Brune, W. H., Tyndall, G. S., Keutsch, F. N., Seinfeld, J. H., and Wennberg, P. O.: Overview of the Focused Isoprene eXperiment at the California Institute of Technology (FIXCIT):

mechanistic chamber studies on the oxidation of biogenic compounds, Atmos. Chem. Phys., 14, 13531-13549, 10.5194/acp-14-13531-2014, 2014.

Odum, J. R., Hoffmann, T., Bowman, F., Collins, D., Flagan, R. C., and Seinfeld, J. H.: Gas/particle partitioning and secondary organic aerosol yields, Environ. Sci. Technol., 30, 10.1021/es950943+, 1996.

Pankow, J. F., and Asher, W. E.: SIMPOL.1: A simple group contribution method for predicting vapor pressures and enthalpies of vaporization of multifunctional organic compounds, Atmos. Chem. Phys., 8, 2773-2796, 10.5194/acp-8-2773-2008, 2008.

Paulot, F., Crounse, J. D., Kjaergaard, H. G., Kroll, J. H., Seinfeld, J. H., and Wennberg, P. O.: Isoprene photooxidation: new insights into the production of acids and organic nitrates, Atmos. Chem. Phys., 9, 1479-1501, 10.5194/acp-9-1479-2009, 2009.

Perring, A. E., Wisthaler, A., Graus, M., Wooldridge, P. J., Lockwood, A. L., Mielke, L. H., Shepson, P. B., Hansel, A., and Cohen, R. C.: A product study of the isoprene+NO_3 reaction, Atmos. Chem. Phys., 9, 4945-4956, 10.5194/acp-9-4945-2009, 2009.

Pratt, K. A., Mielke, L. H., Shepson, P. B., Bryan, A. M., Steiner, A. L., Ortega, J., Daly, R., Helmig, D., Vogel, C. S., Griffith, S., Dusanter, S., Stevens, P. S., and Alaghmand, M.: Contributions of individual reactive biogenic volatile organic compounds to organic nitrates above a mixed forest, Atmos. Chem. Phys., 12, 10125-10143, 10.5194/acp-12-10125-2012, 2012.

Presto, A. A., Hartz, K. E. H., and Donahue, N. M.: Secondary organic aerosol production from terpene ozonolysis. 2. Effect of NOx concentration, Environ. Sci. Technol., 39, 7046-7054, 10.1021/es050400s, 2005.

Pye, H. O. T., Luecken, D. J., Xu, L., Boyd, C. M., Ng, N. L., Baker, K. R., Ayres, B. R., Bash, J. O., Baumann, K., Carter, W. P. L., Edgerton, E. S., Fry, J. L., Hutzell, W. T., Schwede, D. B., and Shepson, P. B.: Modeling the current and future roles of particulate organic nitrates in the Southeastern United States, Environ. Sci. Technol., 49, 14195-14203, 10.1021/acs.est.5b03738, 2015.

Reinnig, M. C., Warnke, J., and Hoffmann, T.: Identification of organic hydroperoxides and hydroperoxy acids in secondary organic aerosol formed during the ozonolysis of different monoterpenes and sesquiterpenes by on-line analysis using atmospheric pressure chemical ionization ion trap mass spectrometry, Rapid Commun. Mass Sp., 23, 1735-1741, 10.1002/rcm.4065, 2009.

Riipinen, I., Yli-Juuti, T., Pierce, J. R., Petaja, T., Worsnop, D. R., Kulmala, M., and Donahue, N. M.: The contribution of organics to atmospheric nanoparticle growth, Nat. Geosci., 5, 453-458, 10.1038/ngeo1499, 2012.

Rindelaub, J. D., McAvey, K. M., and Shepson, P. B.: The photochemical production of organic nitrates from alpha-pinene and loss via acid-dependent particle phase hydrolysis, Atmos. Environ., 100, 193-201, 10.1016/j.atmosenv.2014.10.010, 2015a.

906 Rindelaub, J. D., McAvey, K. M., and Shepson, P. B.: The photochemical production of organic
907 nitrates from alpha-pinene and loss via acid-dependence particle phase hydrolysis, Atmos.
908 Environ., 100, 193-201, 10.1016/j.atmosenv.2014.11.010, 2015b.

909 Rindelaub, J. D., Borca, C. H., Hostetler, M. A., Slade, J. H., Lipton, M. A., Slipchenko, L. V.,
910 and Shepson, P. B.: The acid-catalyzed hydrolysis of an α-pinene-derived organic nitrate: kinetics,
911 products, reaction mechanisms, and atmospheric impact, Atmos. Chem. Phys., 16, 15425-15432,
912 10.5194/acp-16-15425-2016, 2016.

913 Roberts, J. M.: The atmospheric chemistry of organic nitrates, Atmos. Environ., 24A, 243-287,
914 1990.

915 Rollins, A. W., Fry, J. L., Hunter, J. F., Kroll, J. H., Worsnop, D. R., Singaram, S. W., and Cohen,
916 R. C.: Elemental analysis of aerosol organic nitrates with electron ionization high-resolution mass
917 spectrometry, Atmos. Meas. Tech., 3, 301-310, 10.5194/amt-3-301-2010, 2010a.

918 Rollins, A. W., Smith, J. D., Wilson, K. R., and Cohen, R. C.: Real time in situ detection of organic
919 nitrates in atmospheric aerosols, Environ. Sci. Technol., 44, 5540-5545, 10.1021/es100926x,
920 2010b.

921 Rollins, A. W., Browne, E. C., Min, K. E., Pusede, S. E., Wooldridge, P. J., Gentner, D. R.,
922 Goldstein, A. H., Liu, S., Day, D. A., Russell, L. M., and Cohen, R. C.: Evidence for NO_x control
923 over nighttime SOA formation, Science, 337, 10.1126/science.1221520, 2012.

924 Russell, L. M., Bahadur, R., and Ziemann, P. J.: Identifying organic aerosol sources by comparing
925 functional group composition in chamber and atmospheric particles, Proc. Nat. Acad. Sci., 108,
926 3516-3521, 10.1073/pnas.1006461108, 2011.

927 Saunders, S. M., Jenkin, M. E., Derwent, R. G., and Pilling, M. J.: Protocol for the development
928 of the Master Chemical Mechanism, MCM v3 (Part A): tropospheric degradation of non-aromatic
929 volatile organic compounds, Atmos. Chem. Phys., 3, 161-180, 10.5194/acp-3-161-2003, 2003.

930 Schwantes, R. H., Teng, A. P., Nguyen, T. B., Coggon, M. M., Crounse, J. D., St Clair, J. M.,
931 Zhang, X., Schilling, K. A., Seinfeld, J. H., and Wennberg, P. O.: Isoprene NO3 Oxidation
932 Products from the RO2 + HO2 Pathway, J. Phys. Chem. A, 119, 10158-10171,
933 10.1021/acs.jpca.5b06355, 2015.

934 Shepson, P. B., Mackay, E., and Muthuramu, K.: Henry's law constants and removal processes for
935 several atmospheric beta-hydroxy alkyl nitrates, Environ. Sci. Technol., 30, 3618-3623,
936 10.1021/Es960538y, 1996.

937 Shiraiwa, M., and Seinfeld, J. H.: Equilibration timescale of atmospheric secondary organic
938 aerosol partitioning, Geophys. Res. Lett., 39, 10.1029/2012gl054008, 2012.

939 Song, C., Na, K. S., and Cocker, D. R.: Impact of the hydrocarbon to NOx ratio on secondary
940 organic aerosol formation, Environ. Sci. Technol., 39, 3143-3149, 10.1021/es0493244, 2005.

941 Spittler, M., Barnes, I., Bejan, I., Brockmann, K. J., Benter, T., and Wirtz, K.: Reactions of NO3
942 radicals with limonene and alpha-pinene: Product and SOA formation, Atmos. Environ., 40, S116-
943 S127, 10.1016/j.atmosenv.2005.09.093, 2006.

944 Spracklen, D. V., Carslaw, K. S., Pöschl, U., Rap, A., and Forster, P. M.: Global cloud
945 condensation nuclei influenced by carbonaceous combustion aerosol, Atmos. Chem. Phys., 11,
946 9067-9087, 10.5194/acp-11-9067-2011, 2011.

947 Squire, O. J., Archibald, A. T., Griffiths, P. T., Jenkin, M. E., Smith, D., and Pyle, J. A.: Influence
948 of isoprene chemical mechanisms on modelled changes in tropospheric ozone due to climate and
949 land use over the 21st century, Atmos. Chem. Phys., 15, 5123-5143, 10.5194/acp-15-5123-2015,
950 2015.

951 Stocker, T. F., Qin, D., Plattner, G. K., Tignor, M., Allen, S. K., Boschung, J., Nauels, A., Xia, Y.,
952 Bex, V., and Midgley, P. M.: Climate Change 2013: the Physical Science Basis, contribution of
953 Working Group 1 to the Fifth Assessment Report of the Intergovernmental Panel on Climate
954 Change, Cambridge University Press, Cambridge, UK and New York, NY, USA, 2013.

955 Suda, S. R., Petters, M. D., Yeh, G. K., Strollo, C., Matsunaga, A., Faulhaber, A., Ziemann, P. J.,
956 Prenni, A. J., Carrico, C. M., Sullivan, R. C., and Kreidenweis, S. M.: Influence of functional
957 groups on organic aerosol cloud condensation nucleus activity, Environ. Sci. Technol., 48, 10182-
958 10190, 10.1021/es502147y, 2014.

959 Surratt, J. D., Gomez-Gonzalez, Y., Chan, A. W. H., Vermeylen, R., Shahgholi, M., and
960 Kleindienst, T. E.: Organosulfate formation in biogenic secondary organic aerosol, J. Phys. Chem.
961 A, 112, 8345-8378, 10.1021/jp802310p, 2008.

962 Tan, D., Faloona, I., Simpas, J. B., Brune, W., Shepson, P. B., Couch, T. L., Sumner, A. L., Carroll,
963 M. A., Thornberry, T., Apel, E., Riemer, D., and Stockwell, W.: HOx budgets in a deciduous
964 forest: Results from the PROPHET summer 1998 campaign, J. Geophys. Res.-Atmos., 106, 24407-
965 24427, Doi 10.1029/2001jd900016, 2001.

966 Tsigaridis, K., and Kanakidou, M.: Secondary organic aerosol importance in the future
967 atmosphere, Atmos. Environ., 41, 4682-4692, 10.1016/j.atmosenv.2007.03.045, 2007.

968 Valorso, R., Aumont, B., Camredon, M., Raventos-Duran, T., Mouchel-Vallon, C., Ng, N. L.,
969 Seinfeld, J. H., Lee-Taylor, J., and Madronich, S.: Explicit modelling of SOA formation from α-
970 pinene photooxidation: sensitivity to vapour pressure estimation, Atmos. Chem. Phys., 11, 6895-
971 6910, 10.5194/acp-11-6895-2011, 2011.

972 Vereecken, L., and Peeters, J.: Decomposition of substituted alkoxy radical-part I: A generalized
973 structure-activity relationship for reaction barrier heights, Phys. Chem. Chem. Phys., 11, 9062-
974 9074, 10.1039/B909712K, 2009.

975 von Schneidemesser, E., Monks, P. S., Allan, J. D., Bruhwiler, L., Forster, P., Fowler, D., Lauer,
976 A., Morgan, W. T., Paasonen, P., Righi, M., Sindelarova, K., and Sutton, M. A.: Chemistry and
977 the linkages between air quality and climate change, Chem. Rev., 115, 3856-3897,
978 10.1021/acs.chemrev.5b00089, 2015.

Wangberg, I., Barnes, I., and Becker, K.-H.: Product and mechanistic study of the reaction of NO3 radicals with alpha-pinene, Environ. Sci. Technol., 31, 2130-2135, 10.1021/es960958n, 1997.

Xiong, F., McAvey, K. M., Pratt, K. A., Groff, C. J., Hostetler, M. A., Lipton, M. A., Starn, T. K., Seeley, J. V., Bertman, S. B., Teng, A. P., Crounse, J. D., Nguyen, T. B., Wennberg, P. O., Misztal, P. K., Goldstein, A. H., Guenther, A. B., Koss, A. R., Olson, K. F., de Gouw, J. A., Baumann, K., Edgerton, E. S., Feiner, P. A., Zhang, L., Miller, D. O., Brune, W. H., and Shepson, P. B.: Observations of isoprene hydroxynitrates in the southeastern United States and implications for the fate of NO_x, Atmos. Chem. Phys., 15, 11257-11272, 10.5194/acp-15-11257-2015, 2015.

Xiong, F. L. Z., Borca, C. H., Slipchenko, L. V., and Shepson, P. B.: Photochemical degradation of isoprene-derived 4,1-nitrooxy enal, Atmos. Chem. Phys., 16, 5595-5610, 10.5194/acp-16-5595-2016, 2016.

Xu, L., Suresh, S., Guo, H., Weber, R. J., and Ng, N. L.: Aerosol characterization over the southeastern United States using high-resolution aerosol mass spectrometry: spatial and seasonal variation of aerosol composition and sources with a focus on organic nitrates, Atmos. Chem. Phys., 15, 7307-7336, 10.5194/acp-15-7307-2015, 2015.

Yeh, G. K., and Ziemann, P. J.: Alkyl nitrate formation from the reactions of C_8-C_{14} *n*-alkanes with OH radicals in the presence of NO_x: measured yields with essential corrections for gas-wall partitioning, J. Phys. Chem. A, 118, 8147-8157, 10.1021/jp500631v, 2014.

Zhang, X., Cappa, C. D., Jathar, S. H., Mcvay, R. C., Ensberg, J. J., Kleeman, M. J., and Seinfeld, J. H.: Influence of vapor wall loss in laboratory chambers on yields of secondary organic aerosol, Proc. Nat. Acad. Sci., 111, 5802-5807, 10.1073/pnas.1404727111, 2014.

Ziemann, P. J., and Atkinson, R.: Kinetics, products, and mechanisms of secondary organic aerosol formation, Chem. Soc. Rev., 41, 6582-6605, 10.1039/C2CS35122F, 2012.